UNIVERSITAT POLITÈCNICA DE VALÈNCIA

UNIVERSITAT POLITÈCNICA DE VALÈNCIA

Plant Molecular and Cellular Biology Joint Research Institute (IBMCP)

Gibberellins transport regulation in the apical stem cells population

Master's Thesis

Master's Degree in Plant Molecular and Cellular Biotechnology

AUTHOR: Jurado García, Silvia

Tutor: Vera Sirera, Francisco José

Experimental director: SERRANO MISLATA, ANTONIO

ACADEMIC YEAR: 2023/2024

UNIVERSITAT POLITÈCNICA DE VALÈNCIA

CSIC

CONSEJO SUPERIOR DE INVESTIGACIONES CIENTÍFICAS

Instituto de Biología Molecular y Celular de Plantas

Gibberellins transport regulation in the apical stem cells population

Master's Thesis

Author: Silvia Jurado García

Scientific director: Antonio Serrano Mislata

Academic director: Francisco Vera Sirera

Academic year: 2023/2024

I would like to express my gratitude in this work to all those who have helped me make it possible.

Firstly, I want to thank Antonio for giving me this great opportunity and for constantly assisting me in improving this work. I would also like to express my gratitude to Vicente and Asier for providing their assistance in some experiments.

Secondly, I want to extend my thanks to the Plant Signalling group for their kindness and support.

And lastly, I want to thank my family and friends for always encouraging and supporting me.

ABSTRACT

The shoot apical meristem (SAM) harbours a population of pluripotent stem cells that gives rise to all the aerial organs of the plant. The balance between cell division and cell growth must be precisely regulated in the SAM to maintain a stable population of stem cells while continuously supplying new cells for organ formation. This balance relies on the accurate interpretation of environmental signals and endogenous signals from the plant, which are transmitted to the SAM through different hormonal signalling pathways, such as that of gibberellins (GAs).

Under favourable environmental conditions, high levels of GAs promote flowering and plant growth. However, an excess of GAs can disrupt cellular activity in the SAM, consequently affecting its ability to produce new organs. The transcription factor BREVIPEDICELLUS (BP) is a candidate to control GA levels in the SAM in response to environmental fluctuations.

Previous work of the group showed that the cells of the SAM of loss-of-function *bp* mutants are hypersensitive to high levels of GAs, abnormally increasing in size. Additionally, treatments with exogenous GA showed that the entry of GA into the bp SAM was facilitated. Transcriptomic analyses revealed that the expression of *NPF4.3*, a gene encoding a hormone transporter, is significantly induced in *bp* mutants.

The overall objective of this work was to explore the hypothesis that BP controls the entry of GAs into the SAM through the transcriptional regulation of *NPF4.3*.

Here we provide evidence to support this hypothesis. Thus, the *NPF4.3* gene is expressed in the SAM domain. Moreover, the NPF4.3 protein locates at the plasma membrane in plant cells and it is able to transport GAs in yeast. In Arabidopsis, *NPF4.3* over-expression lines were hypersensitive to the exogenous application of GAs, while *npf4.3* mutants showed reduced SAM activity.

On the other hand, reporter analyses showed that GA levels are higher in bp SAM cells with respect to the wt. bp mutants flowered earlier under long-day conditions, but SAM activity was reduced and was more susceptible to drought stress.

In summary, this work reveals *NPF4.3* as a novel regulator of SAM activity, that may act downstream of BP to fine-tune GA content in the SAM region and thus SAM activity.

Key words: shoot apical meristem; gibberellins; BP; NPF4.3; Arabidopsis

RESUMEN

El meristemo apical de tallo (SAM) alberga una población de células madre pluripotentes que da origen a todos los órganos de la parte aérea de la planta. El balance entre la división celular y el crecimiento celular debe regularse con precisión en el SAM para mantener una población estable de células madre y suministrar continuamente nuevas células para la formación de órganos. Este balance depende de la precisa interpretación de señales ambientales y señales endógenas de la planta, las cuales se transmiten al SAM a través de diferentes vías de señalización hormonal, como la de las giberelinas (GAs).

En condiciones ambientales favorables, niveles altos de GAs estimulan la floración y el crecimiento de la planta. Sin embargo, un exceso de GAs puede perturbar la actividad celular en el SAM, afectando su capacidad para producir nuevos órganos. Un candidato para la regulación de los niveles de GAs en el SAM en respuesta a fluctuaciones ambientales es el factor de transcripción BREVIPEDICELLUS (BP).

Trabajos previos del grupo han mostrado que las células del SAM de los mutantes de pérdida de función *bp* son hipersensibles a niveles elevados de GAs, aumentando anormalmente de tamaño. Además, tratamientos con GAs exógenas mostraron que la entrada de GAs en el SAM de *bp* estaba facilitada. Análisis transcriptómicos mostraron que la expresión de *NPF4.3*, un gen que codifica un transportador de hormonas se induce significativamente en mutantes *bp*.

El objetivo general de este trabajo fue explorar la hipótesis de que BP controla la entrada de GAs en el SAM mediante la regulación transcripcional de *NPF4.3*.

Aquí proporcionamos evidencias para respaldar esta hipótesis. El gen *NPF4.3* se expresa en el dominio del SAM. Además, la proteína NPF4.3 se localiza en la membrana plasmática de las células vegetales y es capaz de transportar GAs en levadura. En Arabidopsis, las líneas que sobreexpresan *NPF4.3* eran hipersensibles a la aplicación exógena de GAs, mientras que los mutantes npf4.3 mostraron una actividad reducida en el SAM.

Por otro lado, los análisis de reporteros mostraron que los niveles de GAs son más altos en las células del SAM de *bp* en comparación con las de wt. Los mutantes *bp* florecieron antes bajo condiciones de día largo, pero la actividad del SAM se redujo y fue más susceptible al estrés por sequía.

En resumen, este trabajo revela a *NPF4.3* como un nuevo regulador de la actividad del SAM, que puede actuar aguas abajo de BP para ajustar con precisión el contenido de GAs en la región del SAM y, por lo tanto, la actividad del SAM.

Palabras clave: meristemo apical del tallo; giberelinas; BP; NPF4.3; Arabidopsis

INDEX

1. INTRODUCTION

1.1. The shoot apical meristem

The shoot apical meristem (SAM) is a specialised organ at the shoot apex of the inflorescence that provides an appropriate environment for the activity of the apical stem cells niche. Therefore, the SAM plays a crucial role in the growth and development of all the tissues and organs of the aerial part of the plant, including fruits and seeds (Traas & Vernoux, 2002). Therefore, understanding the molecular and physiological processes underlying SAM activity will provide insights of interest to improve crops yield (Li et al., 2021)

1.1.1.Structure

The SAM can be divided into three clonally different cell layers (L1-L3) (Figure 1); the first two (L1 and L2) present anticlinal cell divisions to give rise to the epidermis (L1) and to internal tissues and the germline (L2). The third layer (L3), which presents randomly orientated cell divisions, also gives rise to the inner tissues and to the vasculature (Ha et al., 2010; Gaillochet et al., 2015)

Three functionally distinct domains or zones can also be differentiated in the SAM (Figure 1). The central zone (CZ) includes the population of stem cells. These cells divide asymmetrically to replenish the stem cells niche while providing new cells for differentiation in the peripheral (PZ) and rib zones (RZ). Cells in the PZ, which flanks the CZ, divide faster and progressively differentiate to get incorporated to the formation of new organs like leaves or flower primordia. The RZ is found further inside the meristem under the central zone and is responsible for giving rise to the pith tissues of the stem.

Between the CZ and the RZ, we find an essential region of cells known as the organising center (OC) that acts as a specialised niche, supporting the stem cell reservoir above it.

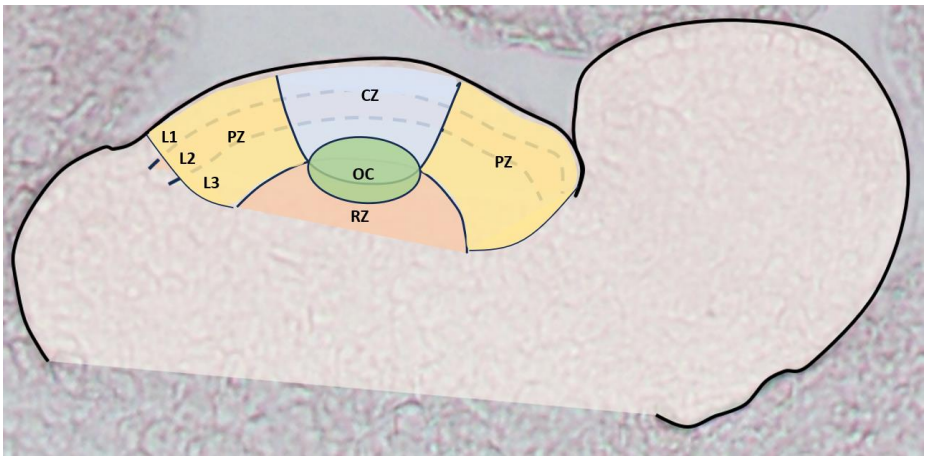

Figure 1: Schematic representation of the clonal cell layers (L1-L3) and functional regions of the SAM (**CZ** = "central zone", **PZ** = "peripheral zone", **RZ** = "rib zone" and **OC** = "organizing center")

1.2. SAM regulation

In order to adjust plant inflorescence development to environmental fluctuations, the SAM must uphold a delicate equilibrium between maintaining the stem cells reservoir and providing new cells to trigger organ development. SAM cells plasticity is governed by intricate and interwoven signalling networks. These networks encompass the feedback regulation of genes responsible for meristem maintenance and the transmission of signals related to plant hormones (Ha et al., 2010)

1.2.1.Genetic regulation

The negative regulatory feedback loop formed by CLAVATA3 (CLV3), a small signalling peptide, and WUSCHEL (WUS), a homeodomain transcription factor, is central in the control of cellular activity at the SAM (Figure 2). The *WUS* gene is expressed in the OC. The WUS protein migrates through plasmodesmata to the upper CZ to promote stem cells renewal and proliferation. Stem cells express and secrete CLV3, which is recognised by a kinase receptor system in the underlying cells of the OC to down-regulate *WUS* expression and thus promote stem cells differentiation (Tras & Vernoux, 2002; Gaillochet et al., 2015)

In addition to the WUS-CLV3 system, the activity of the transcription factors of the *KNOX* family is crucial for SAM maintenance and activity. For example, *SHOOTMERISTEMLESS* (*STM*) plays a complementary role to *WUS* in the SAM. While *STM* provides the meristematic identity, *WUS* specifies a specific subset of meristem cells as stem cells. *STM* expression spans the entire SAM domain and inhibits meristem cell differentiation (Jasinski et al.; 2005; Ha et al., 2010)

The suppression of meristem cell differentiation by *STM* occurs mainly via transcriptional repression of the MYB-related genes *ASYMMETRIC LEAVES1* (*AS1*) and *ASYMMETRIC LEAVES2* (*AS2*). *AS1* and *AS2*, in turn, can suppress the expression of *KNOX* genes. The interplay between KNOX transcription factors, expressed in the meristem regions, and *AS1/AS2*, expressed in organ primordia, underscores the significance of these genes in the differentiation of stem cells and the establishment of organ founder cells (Jasinski et al.; 2005; Ha et al., 2010)

Besides *STM*, Arabidopsis harbours three additional class *I KNOX* genes: *KNAT1*, also known as *BREVIPEDICELLUS* (*BP*), *KNAT2* and *KNAT6*. BP acts redundantly with *STM* to maintain meristematic activity (Byrne et al., 2002). BP restricts *KNAT2* and *KNAT6* expression to promote correct inflorescence architecture development (Ragni et al.,2008; Zhao et al., 2015).

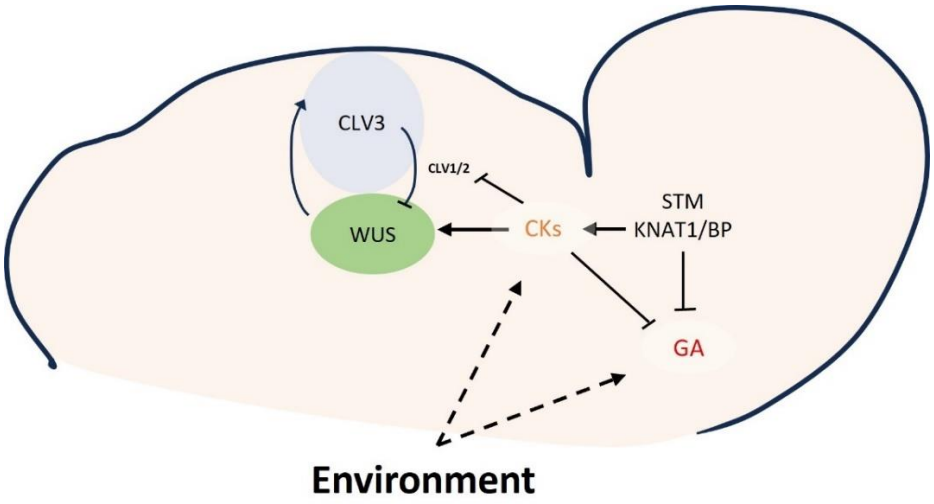

Figure 2: Relationship between the main genetic and hormonal factors that control SAM activity. Arrows represent positive interactions, and blunt lines represent negative interactions.

1.2.2.Hormonal regulation

Phytohormone signalling pathways are crucial for SAM maintenance and activity. Specifically, cytokinins (CK) are believed to be key players in SAM development, acting as positive regulators of cell proliferation and stimulating the division of stem cells. The absence of CK perception leads to a failure in SAM establishment and consequent arrest of vegetative growth, underscoring the essential role of CK in SAM activity. The action of CK in the SAM is regulated at various levels, encompassing biosynthesis, activation, and cellular responses (Ha et al., 2010)

It has been shown that there is a peak of CK signalling in the OC, coinciding with the expression domain of *WUS* (Figure 2). This aligns with prior observations that the WUS protein inhibits the

transcription of two genes that encode CK signalling repressors, *ARABIDOPSIS RESPONSE REGULATOR7* (*ARR7*) and *ARR15*, suggesting that WUS positively influences the sensitivity of SAM cells to CK. Reciprocally, CKs signalling triggers WUS levels and, in this way, governs the number of stem cells in the meristem. It has also been described that *KNOX1* genes, as *STM*, upregulate CK biosynthesis and, consequently, the CK response in the SAM region (Jasinski et al.; 2005; Ha et al., 2010)

Contrary to CKs, gibberellins (GA) promote cell differentiation, longitudinal cell expansion and cytoskeletal rearrangement in SAM cells. KNOX1 proteins maintain low GA levels in the Arabidopsis SAM by suppressing the expression of *GA20ox* genes, which encode enzymes involved in a rate-limiting step of GA biosynthesis (Hay et al., 2002). *KNOX* genes also directly trigger the expression of the *GA2ox* genes, which encode GA-inactivating enzymes (Jasinski et al.; 2005). Given that *GA2ox* genes are mainly expressed at the SAM periphery, their activation by KNOX1 proteins might impede the entry of active GAs from leaf primordia into the SAM. Hence, *KNOX1* genes promote SAM activity by maintaining a low GAs-high CKs environment that favours cell proliferation (Figure 3) (Jasinski et al.,2005).

Auxin levels are normally kept low in the SAM central region but are required to maintain the activity of the stem cells niche. In contrast, periodic auxin maxima drive organ initiation in the SAM periphery. It was reported that auxin negatively regulates the CK signalling inhibitors *ARR7* and *ARR15* through the action of the *MONOPTEROS/AUXIN RESPONSE FACTOR5* (*MP/ARF5*) transcription factor, indicating a crosstalk between CK and auxin in the regulation of stem cells activity and SAM development (Shi & Vernoux, 2019)

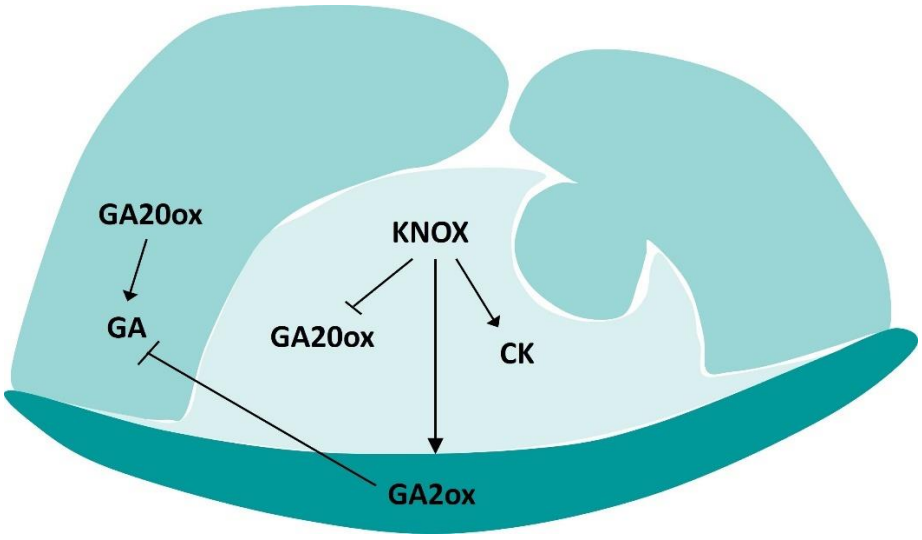

Figure 3: KNOX regulation of CK and GA signalling in the SAM region. Arrows represent positive interaction and blunted lines represent negative interaction. (Modified from Jasinski et al.,2005)

1.2.3.Environmental regulation

During plant development, the morphological and structural features of organs exhibit dynamic adaptations in response to environmental fluctuations. This plasticity hinges on the precise regulation of cellular activity in the primary meristems of the plant: SAM, root apical meristem (RAM) and the vascular cambium. Whereas endogenous signals dynamically define the stem cell niches in response to tissue topography, environmental cues are pivotal in facilitating plant adaptation to the environmental fluctuations encountered throughout their life cycle.

CK signalling is one example of the dynamic interplay between plant development and environmental stimuli, with CK biosynthesis being intricately responsive to specific environmental cues. Specifically, the availability of nitrate in root cells and the exposure of leaves to light promote CK signalling. Then, as explained above, CK controls the adjustment of *WUS* expression and, consequently, the modulation of stem cell activity (Shi & Vernoux., 2019)

GA signalling has also been shown to contribute to dynamic changes throughout SAM development, such as an increase in cell number and cell size to promote SAM growth during the floral transition. Two MADS-box transcription factors, SOC1 and SVP, integral components of the gene regulatory network (GRN) that controls the floral transition in response to day-length, regulate the expression of enzymes associated with GA homeostasis in the SAM. These findings underscore the significance of orchestrating the photoperiod and GA dependent pathways to achieve precise morphological transformations in the SAM during its transition from a vegetative to an inflorescence meristem (Kinoshita et al., 2020)

In addition to the pivotal role of plant hormone signalling pathways, the evolutionarily conserved TARGET OF RAPAMYCIN (TOR) kinase complex assumes a critical function in integrating both energy and environmental signals. TOR activity is indispensable for SAM stem cell function, actively participating in the transcriptional regulation of *WUS* (Janocha & Lohmann., 2018).

Plants have developed intricate protective mechanisms to cope with environmental challenges. When exposed to abiotic stresses, plants trigger major changes in shoot and root development, mainly growth reduction which is accompanied by the activation of the secondary metabolism to enhance the levels of osmoprotectant and antioxidant compounds.

Numerous recent studies have endorsed the notion that stemness favours pant tolerance against adverse environmental conditions such as high salinity or drought (Lee et al., 2016; Cai et al., 2022). For example, it has been shown that the R2R3-type MYB96 transcription factor, a key mediator in ABA signalling, connects *STM* expression and drought tolerance. The MYB96

transcription factor binds to the *STM* promoter and triggers its expression in response to drought conditions (Lee et al., 2016). Furthermore, the transcriptome of cells that have experienced stress significantly intersects with that of stem cells or dedifferentiated cells. Preserving the undifferentiated state may empower plant cells to adopt a new cellular fate better suited to environmental challenges (Lee et al., 2016; Cai et al., 2022)

1.3. Our question: how do *KNOX* genes integrate environmental information in SAM cells through the control of the GA signalling pathway?

Previous works extensively described a putative role for *KNOX* genes in the control of GA signalling in the shoot apex. For example, Arabidopsis *STM* can downregulate the expression of the *GA20ox* genes but promote the expression of *GA2ox* genes (Hay et al., 2002; Jasinski et al., 2005) (Figure 3). Tobacco and maize *KNOX* genes have also been shown to directly repress or activate *GA20ox* or *GA2ox* expression, respectively (Sakamoto et al., 2001; Bolduc and Hake, 2009). Therefore, *KNOX* genes have been proposed to maintain a low GA environment in the central region of the shoot apex that is thought to favour SAM activity.

Nevertheless, most of these observations were made in “in vitro” assays or with whole seedlings of *stm* mutants or *STM* overexpression lines, which raises some concerns. Firstly, there is a lack of spatial resolution when working with seedlings. Moreover, the post-embryonic SAM is severely reduced or absent in *stm* mutants (Endrizzi et al., 1996; Long et al., 1996) what impedes a dynamic analysis of how *KNOX* regulate SAM activity at different developmental stages and under different environmental conditions.

For these reasons, we focused on the gene *KNAT1* or *BREVIPEDICELLUS* (*BP*), another member of the class *I KNOX* genes family, which is expressed in the SAM domain, vasculature, peduncles and pedicels (Lincoln et al., 1994; Venglat et al., 2002) . The expression of *KNAT1* in the SAM region decreases concurrently with the transition from vegetative to reproductive development. This transition is marked by alterations in meristem structure, cellular metabolism, and gene expression, so the genes that show altered expression patterns during this transition are likely to play a crucial role in specifying the distinctive developmental programs associated with either the vegetative or inflorescence meristem (Lincoln et al., 1994)

Loss-of-function *bp/knat1* mutants exhibit a drastic reduction in inflorescence growth, shortened florals internodes and pedicels (caused primarily by decreased cell divisions), downward-pointing pedicels, an epidermal stripe of disorganised cells along the stem and vasculature

defects (Figure 4). *BP/KNAT* overexpression induces alterations in leaf shape and elevates CK levels (Venglat et al., 2002)

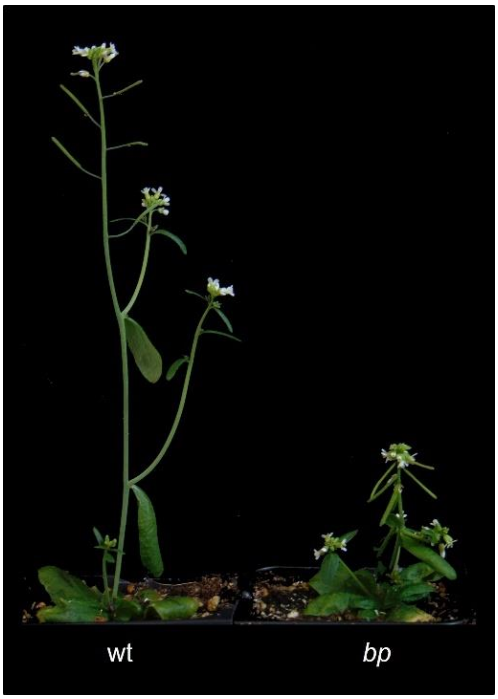

Figure 4: inflorescence architecture of wt and *bp* plants. *bp* mutants show shortened internodes and downward-pointing pedicels.

However, a putative role for *BP/KNAT1* in the SAM has not been analysed with detail yet and many questions about how *KNOX* genes are dynamically regulated in SAM cells remain to be answered.

1.4. Antecedents

In previous work of the group, the cellular structure of the SAM of *bp* mutants was characterised at different stages of the development (vegetative, floral transition and reproductive). This analysis showed that, in comparison to the wt, the *bp* SAM was notably bigger, with bigger cells, at the floral transition stage (Figure 5), when GA levels increase drastically to promote the transition from vegetative to reproductive development (Eriksson et al., 2006). This observation may indicate that the *bp* meristem is more susceptible to high GA levels.

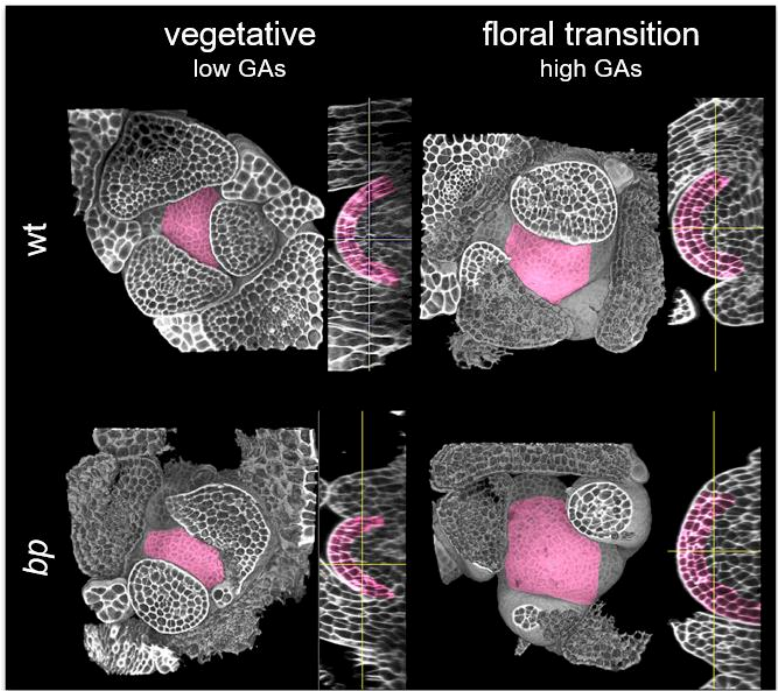

Figure 5: SAM size in wt and *bp* shoot apices in the vegetative and floral transition stages. The SAM domain is false coloured in pink. For each shoot apex, 3D reconstructions from confocal imaging stacks are shown on the left and orthogonal views through the median region are shown on the right.

A possible explanation for this phenotype could be that, as described for *STM*, BP maintains low GA levels in SAM cells. Three non-excluding mechanisms were considered for this: BP inhibition of GA biosynthesis, BP stimulation of GA degradation, or BP restriction of GA entry into the SAM region (Figure 6A). To further explore these possibilities, wt and *bp* seedlings at the vegetative stage were treated with GA_3, a non-degradable GA in Arabidopsis. In mock plants, SAM size was similar between wt and *bp* seedlings. In GA_3-treated plants, only *bp* mutants showed an increase in cell size in the SAM region (Figure 6B). Although the control of GA metabolism by BP cannot be completely discarded, these observations support a novel role for BP in the control of GA entry into SAM cells.

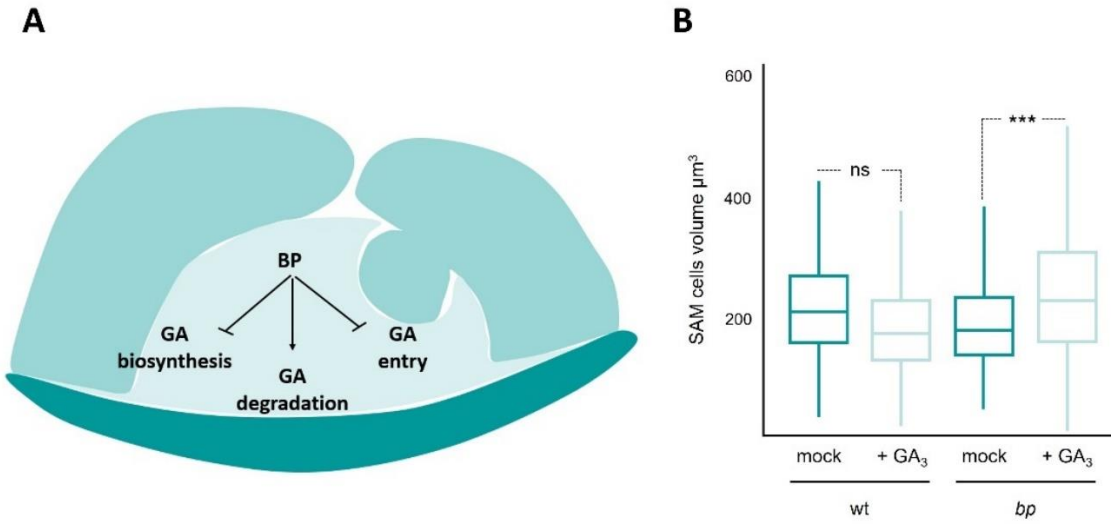

Figure 6: A. Scheme illustrating the possible mechanisms by which BP could control GA content in SAM cells. Arrows indicate positive interaction, and blunted lines indicate negative interaction. **B.** Box plots representing the volume of SAM cells under mock conditions or after treatment with GA_3. Student's t-test; ns: not significant; ***p-value < 0,001

In addition, the analysis of the transcriptome of wt and *bp* shoot apices at the floral transition stage showed that one member of the nitrate transporter 1-peptide transporter (NPF) family, NPF4.3, was significantly upregulated in *bp*. Different NPF proteins have been shown to transport nitrates, sugars, small peptides and phytohormones, such as auxin, abscisic acid and gibberellins (Chiba et al.,2015). Therefore, NPF4.3 was a clear candidate to mediate BP control of SAM growth though the regulation of GA signalling, although the capacity of NPF4.3 to transport GAs had not been demonstrated yet.

1.5. Hypothesis

According to the above-commented results of the group, we hypothesised that BP may be restricting GA entry into SAM cells through the downregulation of the *NPF4.3* gene (Figure 7)

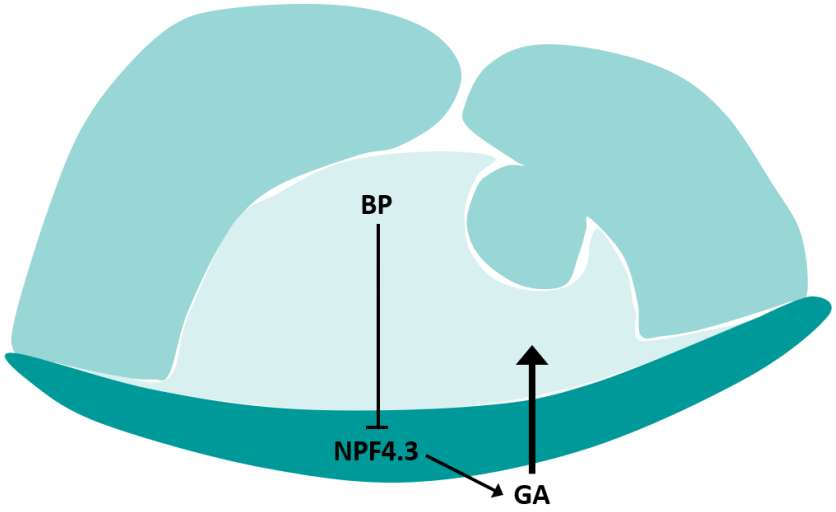

Figure 7: Our working hypothesis for the regulation of GA entry into the SAM domain by BP.

2. OBJECTIVES

Our main objective was to check the hypothesis of BP controlling GA entry into SAM cells through the transcriptional regulation of *NPF4.3*. For this, we planned the following specific objectives:

- Characterisation of the *NPF4.3* gene expression pattern in the shoot apex
- Characterisation of the subcellular localisation of the NPF4.3 protein and testing its capacity to transport GAs
- Analysis of GAs levels in the SAM of *bp-1* mutants
- Analysis of the activity of the SAM of *bp-1* mutants
- Generation and characterization of *npf4.3* loss-of-function mutants by CRISPR/Cas9

3. MATERIALS AND METHODS

3.1. Plant material

Unless otherwise stated, all Arabidopsis plants used in this work were in the in the Landsberg *erecta* (L*er*) background. The *bp-1* mutant has been described previously (Venglat et al., 2002). Reporter lines *RGAp:GFP-RGA* (Silverstone et al., 2001), in the Ler background, and HACR GAI and HACR RGA (Khakhar *et al*., 2018), introgressed three times into Ler, were used to analyse GA content in shoot apices of wt and *bp-1* plants.

A *35S:NFP3.1:YFP* reporter line in the Col background (Tal et al., 2016) was used as a control for root assays with transgenic *35S:NFP4.3:YFP* lines.

For transient transformation assays, *Nicotiana benthamiana* plants were used.

3.1.1.Plant growth in vitro

Seeds were first sterilised with ethanol 70% (v/v) and 0.005% Triton X-100 (v/v) for three minutes, followed by a 96% (v/v) ethanol wash for one minute. All steps were performed in a laminar flow cabinet under sterile conditions. Seeds were then dried on a sterile filter paper and sown onto a Petri dish with a half-strength MS medium.

Seeds were left for 5-7 days at 4º C to favour synchronised germination. Next, plates were transferred to an in vitro culture chamber at 22ºC and long-day photoperiod conditions (16 hours light/8 hours dark) and 100 µmol m^{-2} s^{-1} light intensity.

3.1.2.Plant growth on soil

Seeds (after stratification) or young seedlings coming from plates were grown under controlled conditions of 22º C and long-day (16 hours of light) or short-day (8 hours of light) photoperiods onto a mixture of sphagnum, perlite, and vermiculite (2:1:1), that facilitates Arabidopsis plant growth. Light was provided by cool-white fluorescent lamps at 150 µmol m^{-2} s^{-1}. Plants were regularly watered with tap water.

3.1.3.Plant growth for drought assays

Sterile seeds were stratified in darkness for 7 days at 4ºC in tubes with 0.01% (w/v) agar to help further sowing.

After stratification, seeds were sown onto to 41 mm jiffy pellet disks previously wetted with tap water to reach a weight of 30 gr that corresponded to 60% soil capacity. Plants were grown at 22º C in long-day conditions and 100 µmol m^{-2} s^{-1} light intensity in a Percival growth chamber.

Plants were periodically watered to maintain a pot weight of 25-30 gr until flowering. Then, all pots (Jiffies) were covered with a plastic glass to avoid water evaporation from soil. Control plants were watered to maintain a total weight of 30 gr (weight of the plant/jiffy/glass system plus added tap water) until the end of the experiment. Watering in drought stress plants was uniformly and gradually reduced to reach a total weight of 11 gr (20% soil capacity). Watering was adjusted periodically to keep the 11 gr weight until the end of the experiment.

3.2. Molecular biology techniques

3.2.1.Generation of constructs

3.2.1.1. Generation of *35S:NPF4.3-YFP*

To generate the 35S:NPF4.3-YFP construct, the Gateway (GW) system was employed. The plasmid pENT223:NFP4.3, which contained the NPF4.3 coding sequence (CDS), was amplified with the attB-PCR primers *attB1_NPF4.3_Fw* and *attB2_NPF4.3_Rv* (Table 1). The obtained attB-flanked *NPF4.3* CDS was recombined with the pDONR207 vector through GW BP recombination. pENT207:attB-NPF4.3 was recombined with the pEarlyGate101 plasmid (which contains the 35S promoter and the eYFP protein for C-terminal fusions) through LR recombination to get the *35S:NFP4.3:YFP* construct.

Table 1: Sequence of the primers used to add attB sites to the *NPF4.3* CDS.

Primer name	Sequence (5' to 3')	Position
attB1_NPF4.3_Fw	GGGGACAAGTTTGTACAAAAAAGCAGGCTTCATGGCAGAGATAAACAAACAAAGC	From ATG
attB2_NPF4.3_Rv	GGGGACCACTTTGTACAAGAAAGCTGGGTCAATGTTCTCATCACCCACAACATT	From stop codon

3.2.1.2. Generation of Y2H constructs

Yeast-two hybrid constructs were generated by classical cloning. GID1a was amplified with the primers *EcoRI_GID1a_Fw* and *GID1a_Rev_PstI* (Table 2). The amplified fragment was cloned into the *Eco*RI and *Pst*I restriction sites of the MSC1 of the pBridge vector.

NPF3.1, *NPF4.1* and *NPF4.3* coding sequences were amplified with the primers *NdeI_NPF3.1/4.1/4.3_Fw* and *NPF3.1/4.1/4.3_Rev_HA_NotI* (Table 2). The amplified fragments were cloned into the *Nde*I and *Not*I restriction sites of the MSC2 of the pBridge vector.

Table 2: Sequence of primers used to generate Y2H constructs.

Primer name	Sequence (5' to 3')	Position
EcoRI_GID1a_Fw	TACCGGAATTCATGGCTGCGAGCGATGAAGTTA	From ATG
GID1a_Rev_PstI	AACTGCAGTTAACATTCCGCGTTTACAAACGC	From stop codon
NdeI_NPF3.1_Fw	CCGTACATATGGAGGAGCAAAGCAAGAACAAG	From ATG
NPF3.1_Rev_HA_NotI	AGAATGCGGCCGCTCAGGCATAGTCAGGCACGTCATAAGGATATTCATCAACTAAA CTCCTATTTGACAAC	From stop codon
NdeI_NPF4.1_Fw	CCGTACATATGCAGATTGAGATGGAAGAGAAG	From ATG
NPF4.1_Rev_HA_NotI	AGAATGCGGCCGCTCAGGCATAGTCAGGCACGTCATAAGGATAATATCTTTTCGCC CAGAAAATATAATTAAA	From stop codon
NdeI_NPF4.3_Fw	CCGTACATATGGCAGAGATAAACAAACAAAGC	From ATG
NPF4.3_Rev_HA_NotI	AGAATGCGGCCGCTCAGGCATAGTCAGGCACGTCATAAGGATAAATGTTCTCATCA CCCACAACATTAG	From stop codon

3.2.1.3. Generation of constructs for the edition of the *NPF4.3* gene by CRISPR/Cas9

Guide RNAs (gRNAs) to edit the *NPF4.3* gene (gRNA 14 at the ATG and gRNA 26 at intron 2) were designed with the CRISPR-P v2.0 software http://crispr.hzau.edu.cn/CRISPR2). gRNAs were assembled by amplification of the pCBC-DT1T2 plasmid with primers *CRISPR_NPF4.3_Fw_14* and *CRISPR_NPF4.3_Fw_14-2* and *CRISPR_NPF4.3_Rev_26* and *CRISPR_NPF4.3_Rev_26_2* (Table 3) . gRNAs were cloned into the vector pHEE401 (which contains Cas9 driven by an egg cell-specific promoter-plus a gRNA scaffold for the insertion of target sequences) by Green Gate cloning technology.

3.2.2. Genotyping of CRISPR edited lines

3.2.2.1. Genomic DNA extraction for genotyping

Young and healthy rosette leaves were collected and immediately frozen into liquid nitrogen to facilitate tissue pulverisation. 400 µl of TNES extraction buffer (200 mM Tris-HCl pH 7.5, 250 mM NaCl, 25 mM EDTA, 0.5% SDS) were added to the grinded tissue. Next, samples were briefly vortexed and centrifuged for 1 minute at 13000 rpm. Then, 300 µl of the plant extract was transferred to isopropanol-containing tubes and incubated at room temperature for 5 minutes. Samples were then centrifuged at 13000 rpm for 5 minutes. Isopropanol was then removed, and the precipitated DNA was air-dried for approximately 30 minutes. The DNA was resuspended in 100 µl of Milli-Q water and stored at 4ºC until use.

3.2.2.2. PCR amplification for genotyping *npf4.3* edited lines

Genomic DNA was amplified using the forward primer *NPF4.3_CRISPR_seq_F* and the reverse primer *NPF4.3_CRISPR_seq_R3* (Table 3) using the MyTaq DNA polymerase system. These primers amplify a 1304 bp fragment in the wt allele but a 499 bp fragment in the edited plants. Amplified fragments were analysed by electrophoresis in agarose gels.

Table 3: Sequence of the primers to generate the gRNAs for NPF4.3 edition and of the primers to identify edited plants.

Primer name	Sequence (5' to 3')	Position
CRISPR_NPF4.3_Fw_14	ATATATGGTCTCGATTGTTTGTGTCTTTGTGACAGAGTT	ATG region
CRISPR_NPF4.3_Fw_14_2	TGTTTGTGTCTTTGTGACAGAGTTTTAGAGCTAGAAATAGC	ATG region
CRISPR_NPF4.3_Rev_26	ATTATTGGTCTCGAAACTTTGTGTGTGATCCCATTACAA	2nd intron
CRISPR_NPF4.3_Rev_26_2	AACTTTGTGTGTGATCCCATTACAATCTCTTAGTCGACTCTAC	2nd intron
NPF4.3_CRISPR_seq_F	TTTCTCTCACTCTCTGATCTCC	- 65 bp upstream ATG
NPF4.3_CRISPR_seq_R3	AAGGAGAGTTAGAGCGATAAGC	+ 1217 bp downstream ATG

3.3. *In situ* hybridisation

In situ hybridisation was performed as described by Ferrandiz et al., 2000 with minor modifications. Antisense and sense probes to detect the *NPF4.3* RNA were synthesised and labelled in vitro with digoxigenin-11-UTP using T7 and SP6 polymerases, respectively, from a previously amplified DNA fragment with the primers shown on Table 4.

Table 4: Sequence of the primers used to amplify a fragment of the NPF4.3 CDS.

Primer name	Sequence (5' to 3')	Position
NPF4.3_ISH_Fw_II	ATTTAGGTGACACTATAGGGATTGTTTGTGTCTTTGTGAC	close to ATG
NPF4.3_ISH_Rev	TAATACGACTCACTATAGGGTTATAAGGTTGTTCCCTACTG	2nd exon, 190 bp downstream ATG in cDNA

Shoot apices of wild-type and *bp-1* plants at the vegetative, floral transition and inflorescence stages was fixed in FAE solution (50% ethanol, 3,7% formaldehyde, 5% glacial acetic acid), dehydrated in an ethanol series, embedded in paraffin, and 8 µm sections were obtained with a microtome. Once dewaxed in histoclear and rehydrated in ethanol series, sections were treated in 0.2 M HCl at RT for 20 min, neutralised in ddH_2O, 2 x SSC and ddH_2O for 5 min each one and afterwards were incubated with 1 µg/ml Proteinase K in a solution with 100 mM Tris (pH=8) and 50 mM EDTA (pH=8) at 37ºC for 15 min.

After washing with PBS for 2 min, Proteinase K activity was blocked with 2 mg/ml Glycine in PBS for 2 min and sections were refixed in 4% formaldehyde in PBS for 10 min, followed by another wash with PBS for 2 min and dehydration of the sections with ethanol series.

For hybridisation, a solution containing approximately 100 µg/ml of antisense or sense DIG-labelled RNA probe was applied to the sections and left incubating at 54 ºC overnight. Nex day, sections were washed in 2x SSC and formamide 50% twice for 90 min at the hybridisation temperature.

Prior to the immunodetection, sections were washed in TBS for 5 min, incubated in a blocking solution (0,5% Roche blocking in TBS) for 2 hours and washed in a 1% BSA/0,3% (v/v) Triton X-100/TBS solution for 30 min.

After incubation with a 1% BSA/0,3% (v/v) Triton X-100/TBS solution with 1:3000 AP-conjugated anti-DIG Fab fragment for 2 hours, sections were washed three times in a 1% BSA/0,3% (v/v)

Triton X-100/TBS solution for 20 min each one. Then, sections were washed with detection solution and next incubated in detection solution with the substrates NBT 100 mg/ml and BCIP 50 mg/ml in darkness for 72 hours, when reactions were stopped with ddH_2O.

3.4. Analysis of *NPF4.3-YFP* activity

3.4.1. Transient transformation of *Nicotiana benthamiana* leaves

Suspensions of Agrobacterium tumefaciens strain C58 containing the constructs *35S:NPF3.1-YFP* (positive control, Tal et al., 2016) and *35S:NPF4.3-YFP* were agroinfiltrated in Nicotiana leaves with an agroinfiltration solution containing acetosyringone, $MgCl_2$ and buffer MES.

Discs extracted from agroinfiltrated leaves were observed by confocal microscopy 48 hours after agroinfiltration to check the localisation of the NPF4.3-YFP protein.

3.4.2.*Arabidopsis thaliana* transformation

Wild-type plants were transformed by floral dipping with a suspension of Agrobacterium tumefaciens strain C58 containing the constructs *35S:NPF3.1-YFP* as positive control and *35S:NPF4.3-YFP* in an agroinfiltration solution containing 5% sucrose and 0,05% Silwett L-77.

T2 lines with single-insertion were used to check the localisation of NPF4.3-YFP in root tips by confocal microscopy.

3.4.3.Phenotypic characterisation of *35S:NPF4.3-YFP* overexpression lines

For the root GA response assay, seeds from wt and *35S:NPF4.3-YFP* T2 lines were germinated on 1/2 MS + 1% sucrose plates and transferred to plates supplemented with 5 µM paclobutrazol after 4 days. One day after the transfer, the root length was marked, and 1 µl of 5 µM GA_3 diluted in water was applied to root tips for the three subsequent days. Roots were imaged and measured 10 days later using the ImageJ software.

3.5. Yeast two-hybrid

For the yeast two-hybrid assay, the RGA protein fused to the GAL4 activation domain in the pGADT7 vector and NPF proteins plus the GID1a gibberellins receptor fused to the GAL4 DNA binding domain in the pBridge vector were transformed in the yeast haploid strains Y187 and Y2H-Gold respectively. For yeast transformation, cells were exposed to a 42ºC heat shock in the presence of polyethylene glycol 50% and lithium acetate 1M. Transformants were grown in SD-selective medium without leucine (L) for pGADT7 and without tryptophan (W) for pBridge vector.

Diploid yeasts containing both plasmids were obtained by yeast mating induced by the co-culture of both strains in liquid YPD medium. Diploids were selected in SD -L/W medium plates and grown in liquid SD medium containing L, W, uracil (U) and histidine (H) until saturation.

Saturated cultures were dropped in SD -L/W plates as controls for yeast growth, and in SD -L/W/H + 0,5 μM GA_3 + 0,5 mM 3-AT (a competitive inhibitor of the HIS3 gene) selection plates to check the GA transport.

3.6. Analysis of GA and DELLA reporters by confocal microscopy

Shoot apical meristems from HACR GAI, HACR RGA and DELLA (*RGAp:GFP-RGA*) reporter lines were analysed on a Stelaris Leica SP8 confocal microscope using a water-dipping 40x objective. For this, shoot apices were placed on MS medium plates, and flower buds were removed carefully with tweezers or a needle.

GFP and VENUS were imaged using an argon laser emitting at the wavelength of 488 nm together with a 490-545 nm collection. Z-stacks were acquired with a resolution of 16 bits, a step size of 0.5 μm and a line average of 2. GFP and VENUS gain settings were maintained the same in all the samples analysed for a specific reporter.

Z-stacks were processed with the ImageJ software to obtain maximum intensity projections, orthogonal views and heatmaps of the fluorescence intensity.

3.7. Phenotypic characterisation of *bp* mutants

3.7.1.Flowering time

To monitor flowering time, the total number of rosette and cauline leaves produced in the main inflorescence were counted in wt and *bp-1* plants under long-day and short-day photoperiods until the first floral node was produced.

3.7.2. Analysis of SAM activity

SAM activity was determined by counting the cumulative number of mature flowers and siliques produced in the main inflorescence of plants grown under control and drought conditions. In order to initiate drought treatments, the flowering day was determined as the day on which the floral button was visible to the naked eye on most plants for a particular genotype.

4. RESULTS

4.1. The *NPF4.3* gene is expressed in the SAM domain

To determine the tissue-specific localisation of *NPF4.3*, we performed *in-situ* hybridisation of longitudinal sections of wt and *bp-1* shoot apices at the vegetative, floral transition, and inflorescence developmental stages.

As shown in Figure 8, the *NPF4.3* transcript was mainly detected in the SAM domain, young lateral primordia (either vegetative or floral) in wt and *bp-1* apices in all stages. No signal was detected with the sense probe, supporting that the antisense signal was specific to *NPF4.3*. The *NPF4.3* signal seemed to be slightly higher in *bp-1* sections, supporting our hypothesis that BP could be restricting the entry of GA into SAM cells through the downregulation of *NPF4.3*.

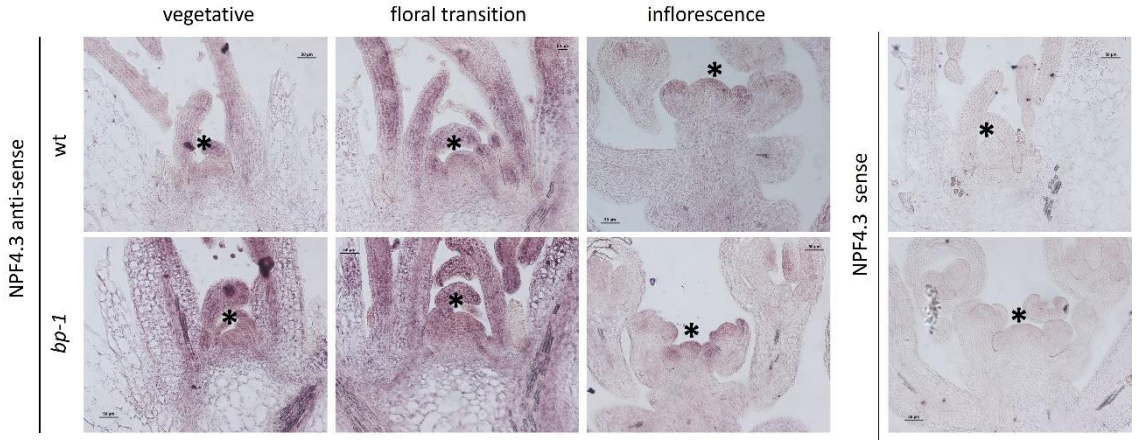

Figure 8: *NPF4.3* gene expression (purple precipitate) in the inflorescence apex of wt and *bp-1* plants at different developmental stages. Sections were hybridised with digoxigenin-labelled antisense and sense probes, as indicated. The SAM domain is marked with an asterisk. Scale bars, 50 µm.

4.2. The NPF4.3 protein can transport GAs

4.2.1.*p35S:NPF4.3-YFP* subcellular localisation in *Nicotiana benthamiana* leaves

Plant hormone transporters are usually located in the plasma membrane, tonoplast or in the endomembrane system (Park et al., 2017). To characterise the subcellular localisation of the NPF4.3 protein by confocal microscopy, we transitory expressed a *p35S:NPF4.3-YFP* construct in *Nicotiana benthamiana* leaves. The NPF4.3-YFP fusion protein was exclusively detected in the plasma membrane (Figure 9), showing a similar pattern to the previously characterised GA transporter NPF3.1 (Tal et al., 2016).

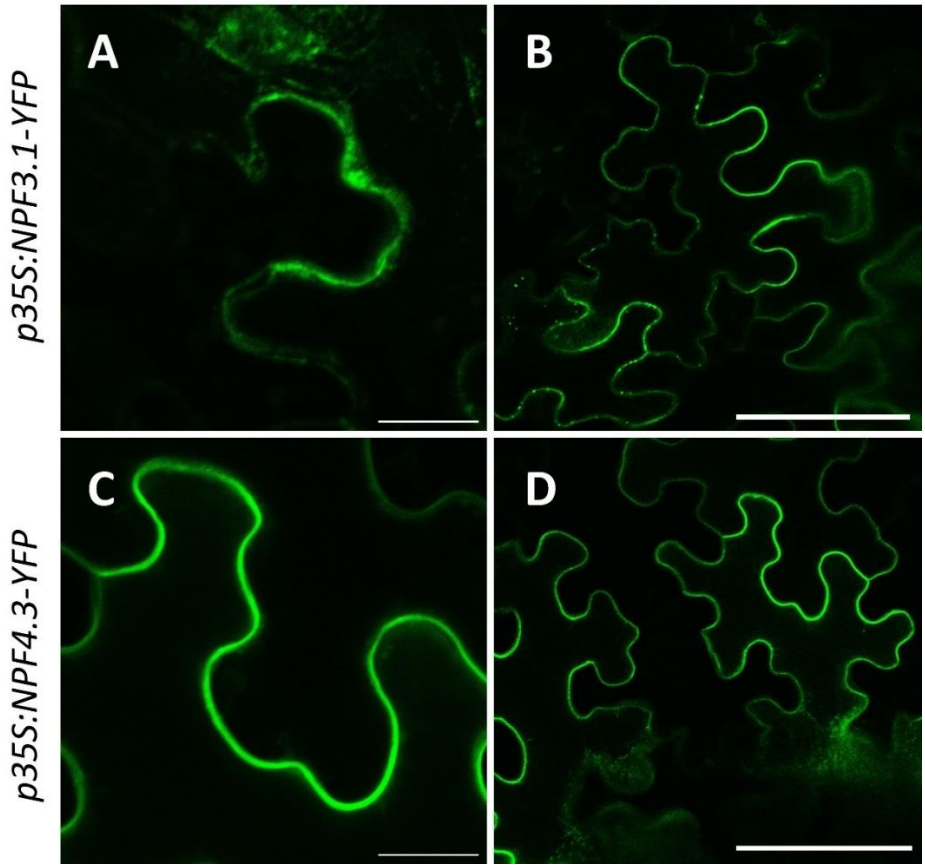

Figure 9: Confocal microscopy images of the subcellular localisation of the NPF3.1-YFP (positive control) and NPF4.3-YFP fusion proteins in tobacco leaves. **(A and C)** Scale bar, 20 µm. **(B and D)** Scale bar, 100 µm.

4.2.2.*p35S:NPF4.3-YFP* subcellular localisation in *Arabidopsis thaliana* roots

To characterise the subcellular localisation of NPF4.3 in Arabidopsis plants, we analysed root tips from *p35S:NPF4.3-YFP* single-insertion T2 lines by confocal microscopy. In contrast to *p35S: NPF3.1-YFP* lines, which were used as controls, we were not able to detect the NPF4.3-YFP fusion protein in the root tip (Figure 10). Given that these lines showed enhanced sensitivity to exogenous GA treatments (see section 4.2.3), this observation may suggest that NPF4.3 protein levels are too low to be detected under normal growing conditions and/or that GAs are needed to increase them.

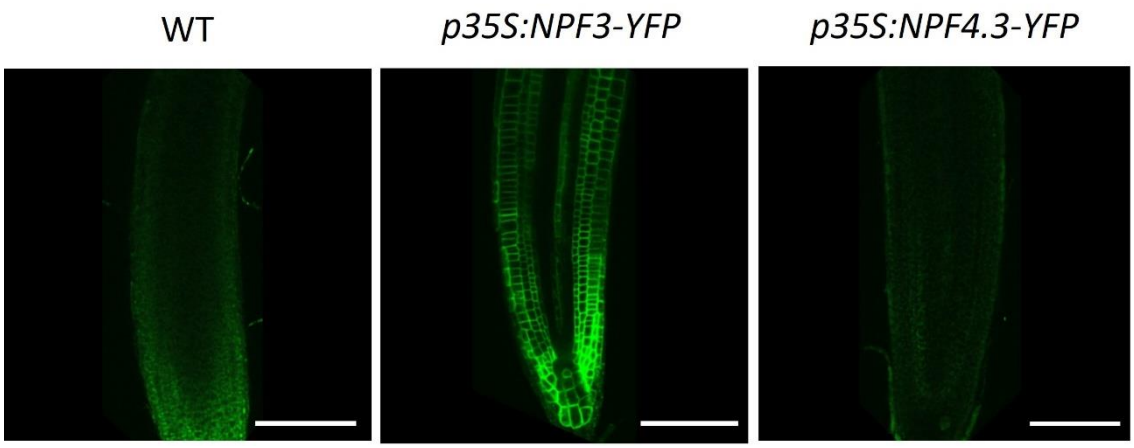

Figure 10: Confocal microscopy images through the median section of root tips from 7-days-old WT, *p35S:NPF3.1-YFP* and *p35S:NPF4.3-YFP* seedlings. Scale bar, 100 µm.

4.2.3.Exogenous GA_3 treatments of *p35S:NPF4.3-YFP* roots

To study a possible role for NPF4.3 on GA transport across plant cells, we analysed a GA-dependent trait, such as root elongation, in wt and *NPF4.3* overexpression lines. We grew seedlings in the presence of paclobutrazol, an inhibitor of plant GA biosynthesis, and then performed exogenous treatments with GA_3.

Three out of four *p35S:NPF4.3-YFP* overexpression lines developed significantly longer roots than wt plants (Figure 11), suggesting that these lines were more sensitive to the exogen application of GAs. This could be explained by the possibility of a facilitated GA movement by NPF4.3.

However, these results contradict what was described for the previously-characterised GA transporter NPF3.1 by Tal et al., 2015. An equivalent experiment showed that root length was reduced in *p35S:NPF3.1-YFP* plants, as occurs in GA-deficient plants, which could be explained by the retention of GAs at the site of synthesis. Therefore, ectopic NPF3.1 would inhibit the movement of GA. According to our observations, the role of NPF4.3 might rather be to favour GA movement to key growth sites.

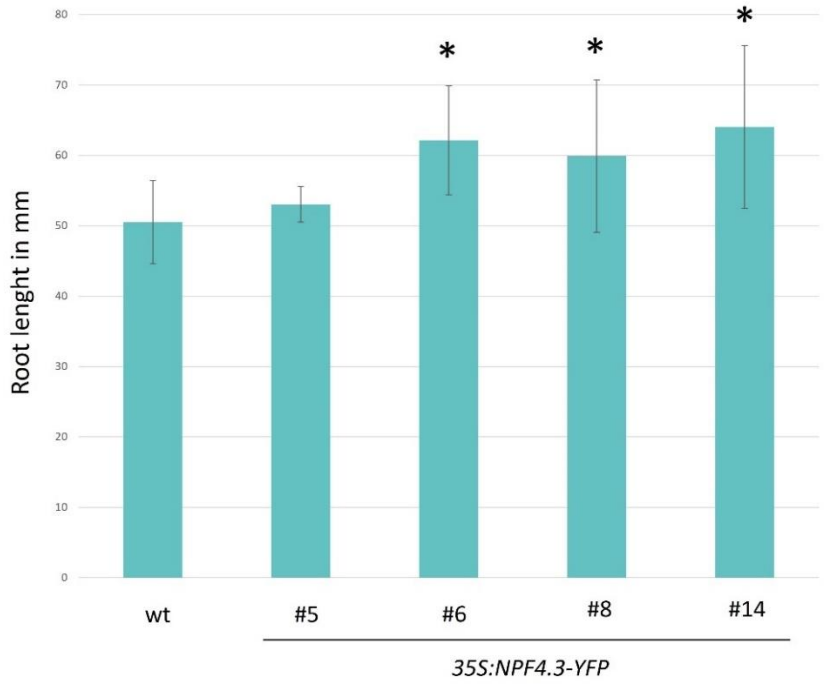

Figure 11: Total root length (mm) of WT and *p35S:NPF4.3-YFP* seedlings grown in the presence of PAC and treated with exogenous GA_3 as indicated in the 3.4.3 section . * = $p < 0,05$. n = 9-10 for each line.

4.2.4.Yeast-two hybrid assays to test the capacity of NPF4.3 to import GAs

Next, we decided to check the capacity of the NPF4.3 protein to import GAs in a heterologous system by a modified yeast-two hybrid approach. DELLA proteins are negative regulators of GA signalling. The interaction of the DELLA protein RGA with the GA receptor (GID1a) is dependent on GA presence (Devière and Achard., 2013Richards et al., 2001).

In this assay, GID1a fused to the GAL4 DNA binding domain (DBD; DBD-GID1a) and RGA fused to the GAL4 activation domain (AD; AD-RGA) were expressed in yeast, in which marker gene *HIS3* (which allows yeast growth on the absence of histidine) expression was activated by the GA-dependent formation of DBD-GID1a/AD-RGA complexes. Under high GA levels in the media, these can enter yeast cells just by passive diffusion, but under low GA levels (0,5 µM GA_3 in this assay), the presence of the transporter makes a difference and helps GA levels to be high enough to promote the interaction and hence yeast growth (Figure 12)

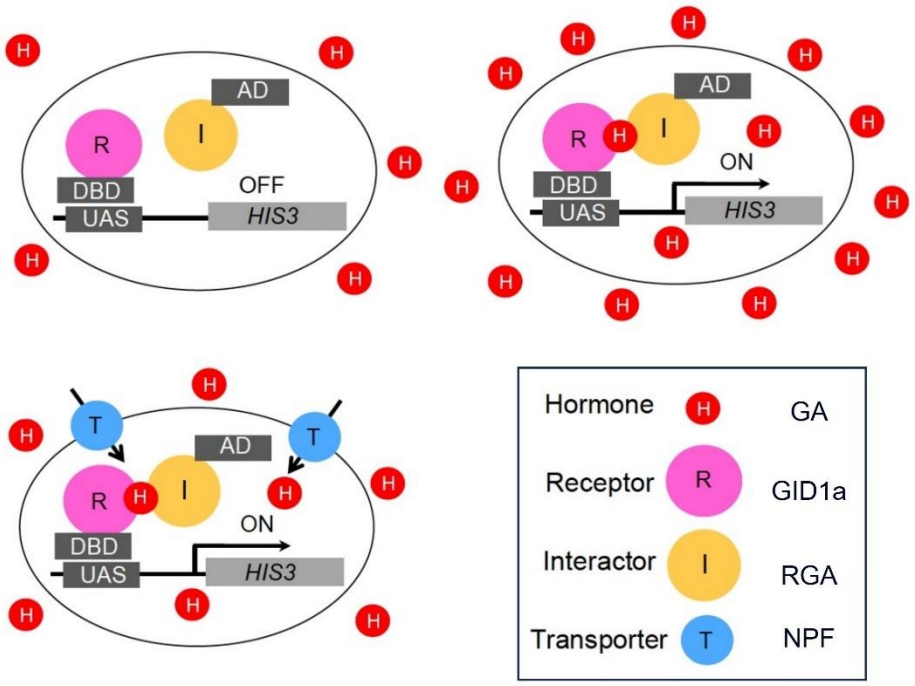

Figure 12: Scheme representing the modified yeast-two hybrid system employed to test the capacity of NPF proteins to transport GAs. AD, activation domain. DBD, DNA binding domain. UAS, GAL4/upstream activating sequence. HIS3, HISTIDINE3 marker gene. ON, *HIS3* transcription activated. OFF, *HIS3* transcription inactivated. Modified from Chiba et al., 2015.

As shown in Figure 13 , all combinations of diploid yeast cells grew similarly in the presence of histidine (+H plates), what indicates that the absence of growth in -H plates should be just reflecting the lack of RGA-GID1a interaction. Yeast growth was never detected in the absence of histidine and/or GAs in the media (negative controls).

In 10^{-3} dilutions from a saturated yeast culture (see material and methods section 3.5), yeast growth was barely observed in the absence of NPF proteins, but clearly favoured in their presence (Figure 13A and 13C).

In 10^{-4} dilutions from the same saturated yeast cultures (Figure 13B and 13D), yeast growth was only reported in the presence of the NPF proteins. Yeast growth was more favoured by NPF4.1 respect to NPF4.3 and NPF3.1, what might reflect different receptor affinities for the hormone.

In summary, yeast assays support that NPF4.3 can transport GA_3 and that different NPF transporters have different affinities for GA_3, as previously reported (Chiba et al., 2015). Future assays will include the analysis of bioactive GAs in Arabidopsis, such as GA_1 or GA_4.

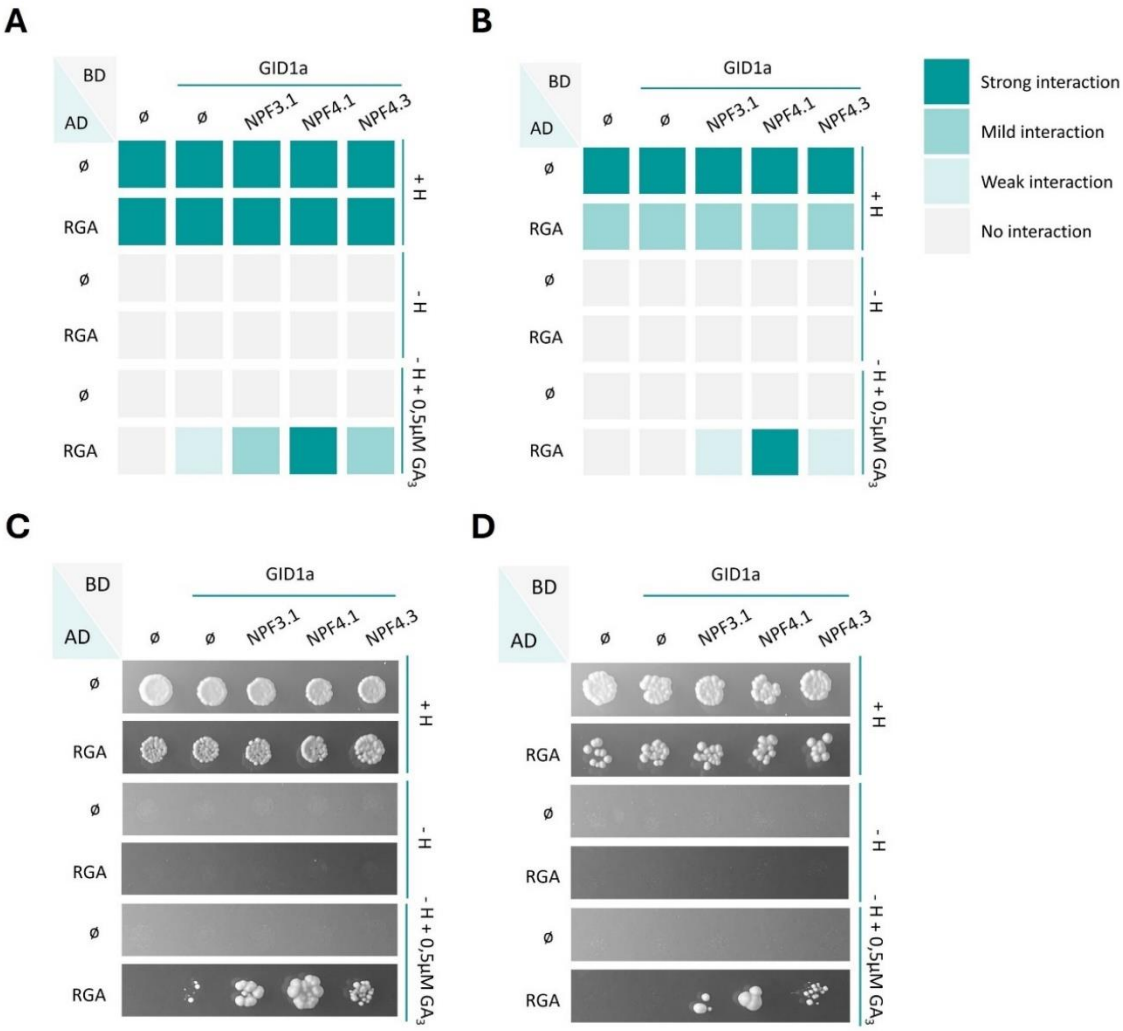

Figure 13: Detection of GA transport activity of NPF proteins by Y2H. Photos were taken five days after inoculation with 10^{-3} (A and C) and 10^{-4} dilutions (B and D) from a saturated grown culture. For each panel, the two upper rows show growth controls in (SD, -Trp, -Ura, +His) plates. The two rows in the middle show growth controls in (SD, -Trp, -Ura, -His) selection plates without GAs. The two lower rows show growth in (SD, -Trp, -Ura, -His) selection plates containing 0,5 µM GA_3 and 0,5 mM 3-AT. AD, activation domain. BD, DNA binding domain. ∅, empty vector.

4.3. Comparative analysis of GA levels in the SAM of wt and *bp* plants

4.3.1. Analysis of GA content by confocal microscopy of fluorescence reporter lines

NPF4.3 is expressed in the SAM domain and yeast assays indicate that NPF4.3 facilitates the entry of GAs into cells. Therefore, we hypothesized that the up-regulation of *NPF4.3* gene expression in *bp* mutant apices might result in higher GA levels in *bp* SAM cells in comparison to the wt.

To compare GA content levels in the SAM at the inflorescence stage, we utilised two different GA-HACR *(hormone-activated Cas9-based repressors)* reporter lines (Khakhar *et al*., 2018) based on the GA-induced degradation of a DELLA protein (RGA or GAI) fused to the TOPLESS

transcriptional repressor, which controls the expression of a fluorescent reporter (Figure 14A). Thus, a higher fluorescence signal indicates a higher GA concentration. These two lines present different dynamic ranges, being the dynamic range of RGA notably wider. Therefore, the GAI-based reporter seems to be more appropriate to detect subtle changes in GA concentrations across different cells and tissues (Figure 14B and 14C).

Complementarily, we also analysed a DELLA reporter line *RGAp:GFP-RGA* (Silverstone et al., 2001). More GAs must degrade more GFP-RGA fusion protein, thereby resulting in lower fluorescence intensity.

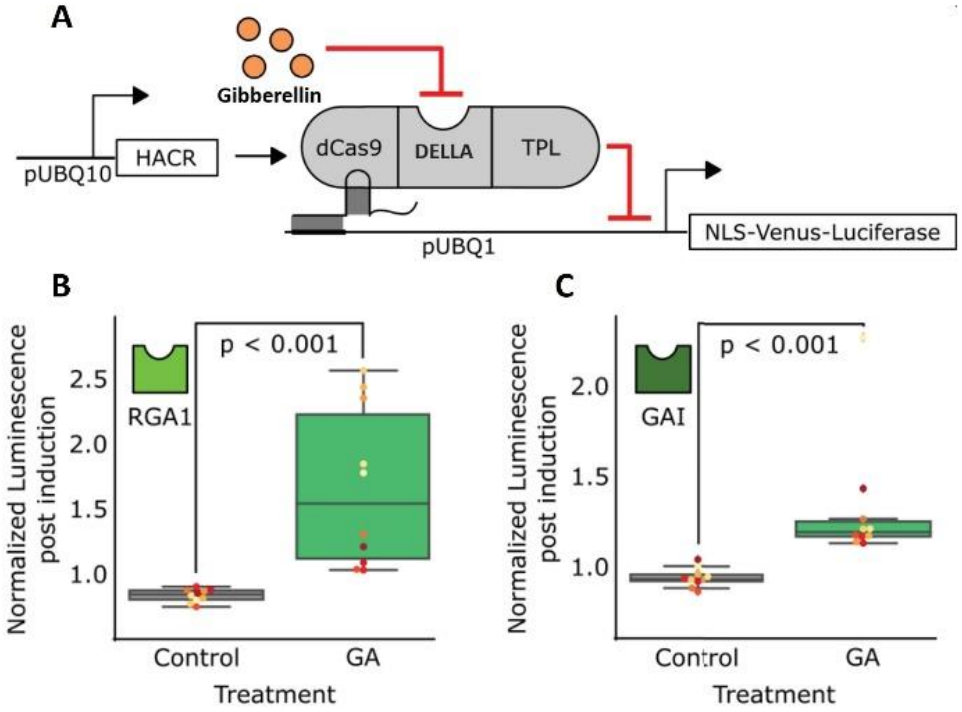

Figure 14: A. Schematic representation of the GA-HACR reporter constructs. **B-C.** Response of transgenic seedlings carrying the GA-HACR constructs to treatment with either control or GAs. The DELLA proteins RGA and GAI were used as the degron in (B) and (C) respectively. Modified from Khakhar *et al.,* 2018.

Confocal images of inflorescence shoot apices at comparable developmental stages showed stronger signal of both GA-HACR reporters in the SAM region of *bp* mutants (Figure 15D and 15E). GAI reporter was below detection threshold in the wt, but a few labelled cells could be detected in *bp* while the RGA reporter was very bright in wt and *bp* shoot cells, being active in the whole SAM region and lateral primordia. Fluoresce intensity also seemed to be higher in *bp* for the RGA reporter.

In line with this, the fluorescence intensity of the DELLA reporter (*RGAp:GFP-RGA*) was lower in the central region of the SAM of the *bp* mutant than in the wt (Figure 15F and 15C). Altogether these observations suggest that endogenous GA levels are higher in the *bp* mutant and, therefore, support the hypothesis that gibberellin entry into SAM cells could be facilitated in *bp*.

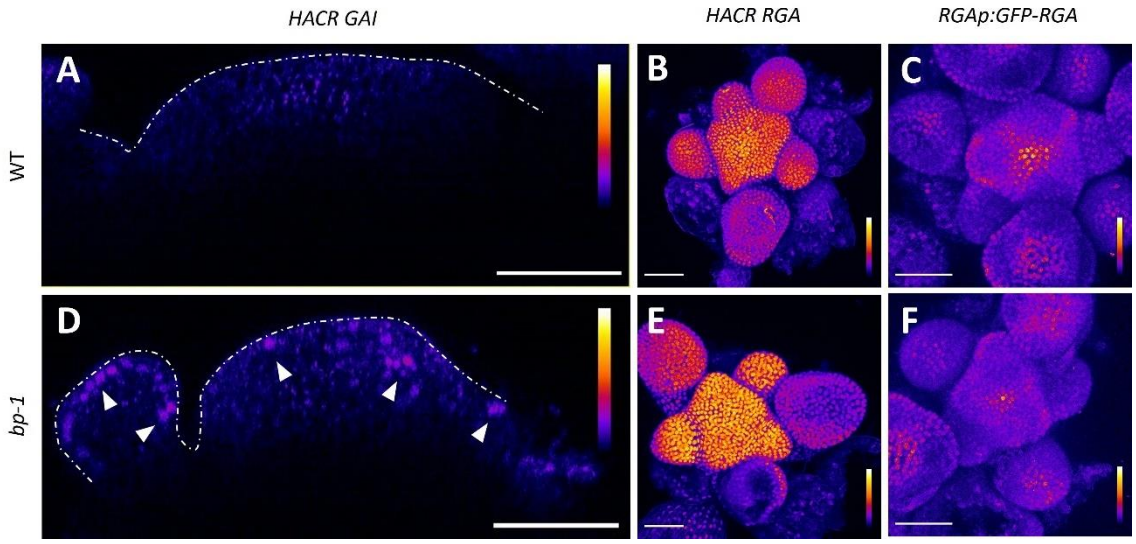

Figure 15: Reporter analysis of GA content in SAM cells. **(A and D)** Orthogonal views of representative wt and bp SAM expressing the GA-HACR GAI reporter. (B-F) 3D reconstitution of confocal images stacks of wt and *bp-1* SAM expressing the GA-HACR RGA **(B and D)** and DELLA *RGAp:RGA-GFP* **(C and F)** reporters. Colour bars for the signal intensity are provided for each panel. Higher fluorescence intensities are in white-yellowish colours and lower fluorescence intensities are in blue-purplish colours. Scale bar, 50 µm.

4.4. Analysis of SAM activity in *bp* mutants

The defects that present the *bp* mutant in the architecture of the inflorescence and in vascular development have been widely described, but possible defects in the structure and/or activity of the SAM have not been studied yet. So, we decided to perform different assays to check how higher GA levels in the *bp* mutant may impact SAM activity.

4.4.1.Flowering time

The floral transition is a developmental process, triggered by GAs among other factors, that takes place in the SAM, which changes from leaf production (vegetative stage) to flower production (reproductive stage). We examined flowering time, determined as the production of leaves, in wt and *bp-1* plants under long-day (LD, 16 h light) and short-day (SD, 8h light) photoperiods.

The *bp* mutant showed early flowering under LD conditions (with an average of 8 leaves in contrast to the average of 10 leaves in the wt, Figure 16). However, there were not significant

differences in flowering time between wt and *bp-1* plants under SD conditions (Figure 16). GA levels are notably higher under LD than SD conditions. Therefore, the earlier flowering of the *bp* mutant only under LD might support the idea that the *bp* SAM is more sensitive to high GA levels.

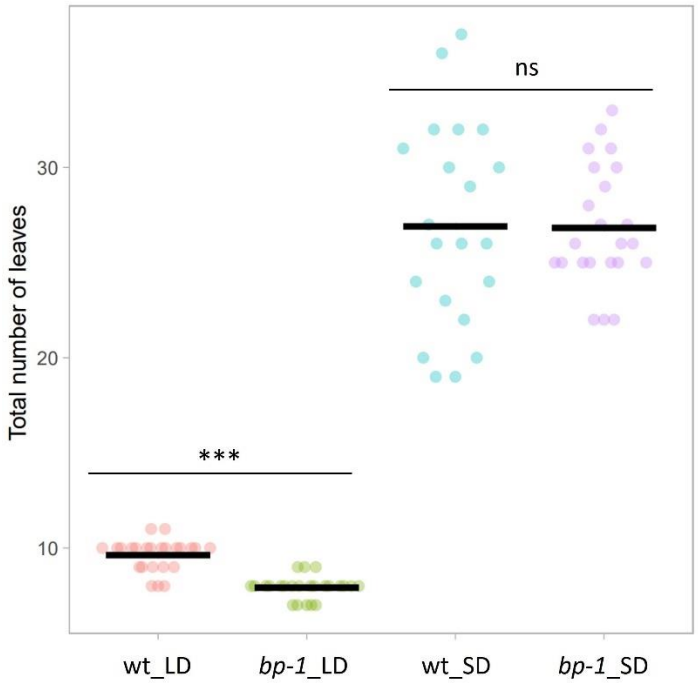

Figure 16: Flowering time of wt and *bp* plants grown under long day (LD) and short-day conditions (SD). Flowering time was estimated as the total number of rosette and cauline leaves. Dots represent independent observations. Thick black lines represent the mean per genotype. n = 24. *** = p < 0,001; ns = not significant.

4.4.2.Flower production

SAM activity can also be monitored as the rate of flower buds production. Previous work shows that enhanced GA signalling boosts flowers production through the degradation of DELLA proteins (Serrano-Mislata et al., 2017). In contrast, higher GAs, and hence less DELLA activity, may make SAM cells more susceptible to abiotic stress conditions. In fact, drought stress has been reported to diminish flower production (Ma et al., 2014; Su et al., 2013).

Therefore, we decided to monitor flower production under well-watered (control) and drought conditions to check in which direction higher GAs influence SAM activity in bp under different environments.

Firstly, we checked water loss in *bp* and wt plants subjected to sustained drought stress. We wanted to assure that both genotypes responded similarly to water deprivation and hence SAM cells were being subjected to comparable stress intensities. For this, we stopped watering after flowering and regularly weighted the pots (which were covered with plastic glasses to avoid

water evaporation from the soil) (Figure 17A) and measured the leaf relative water content (LRWC) (Figure 17B). As shown in Figure 17, both genotypes lost water similarly and the content of water in leaves also decreased similarly as the intensity of the stress increased. Therefore, transpiration responses to decreasing soil water content were comparable in wt and bp plants.

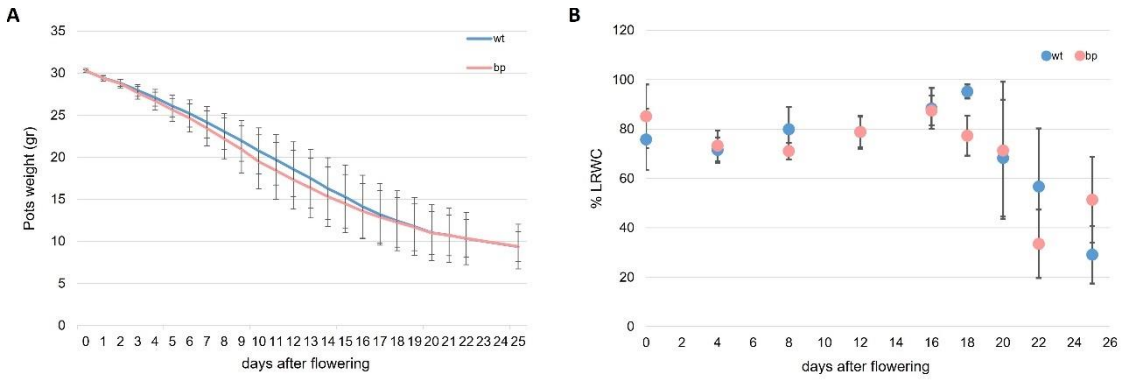

Figure 17: Estimation of plant transpiration in wt and bp plants subjected to drought stress after flowering. (A) Pots weight. n = 15. (B) Relative content of water in rosette leaves. The graph represents the average with the standard deviation of leaves from 3-5 independent plants per genotype and time point.

Under control conditions, the SAM of *bp* mutants produced significantly less flowers (with an average of 21 flowers in contrast to the average of 27 flowers produced in wt, Figure 19A) and stopped flower production earlier (18 days after flowering) than the wt (22 days after flowering) (Figure 19B). In summary, SAM activity and organogenesis rates were impaired in *bp* mutants.

Under drought conditions, *bp-1* also produced less flowers than wt plants (with an average of 17 flowers in contrast to the average of 21 flowers produced in the wt, Figure 19A). Interestingly, the SAM was active for a similar period (18 days in average) in wt and *bp-1* under drought (Figure 19B).

These data show that the *bp* SAM is less active regardless of the growing conditions. However, the impact of *bp* loss-of-function is greater in well-watered plants, at least if we consider the number of days on which the SAM produces new flowers. Drought stress lowers GA levels and low GA levels could make the control of GA entry into the SAM region less relevant.

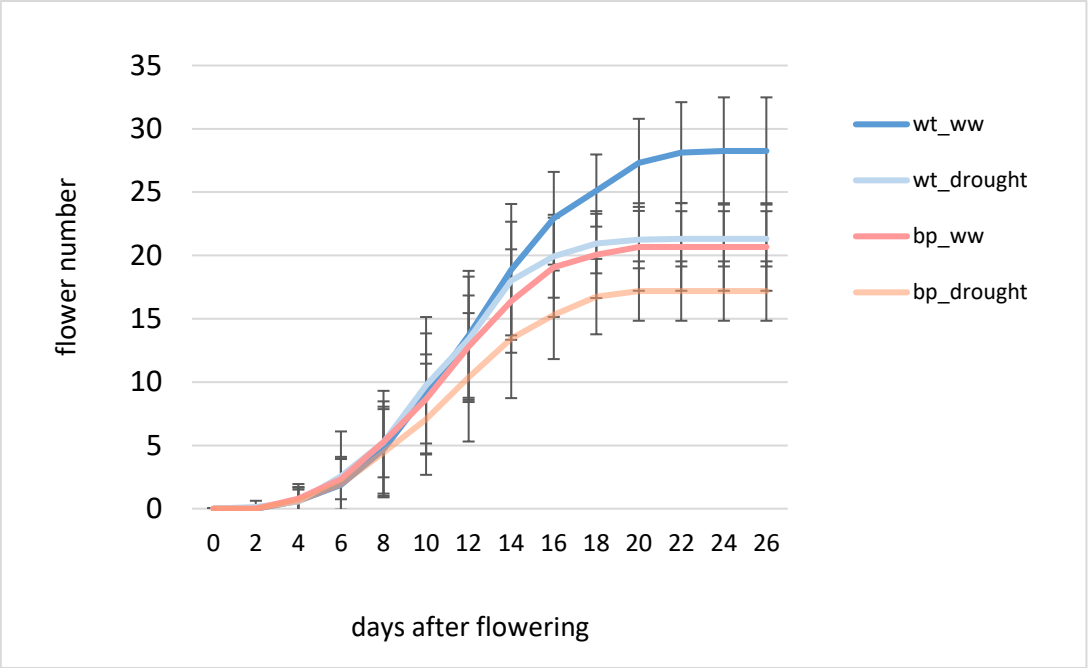

Figure 18: SAM activity represented as the cumulative number of mature flowers in the main inflorescence of wt and *bp-1* plants under control (ww = well-watered) and drought conditions. The flowering day was determined as the day on which the floral button was visible to the naked eye on most plants of a particular genotype. The graphs show the mean and standard deviation of 16 plants per genotype.

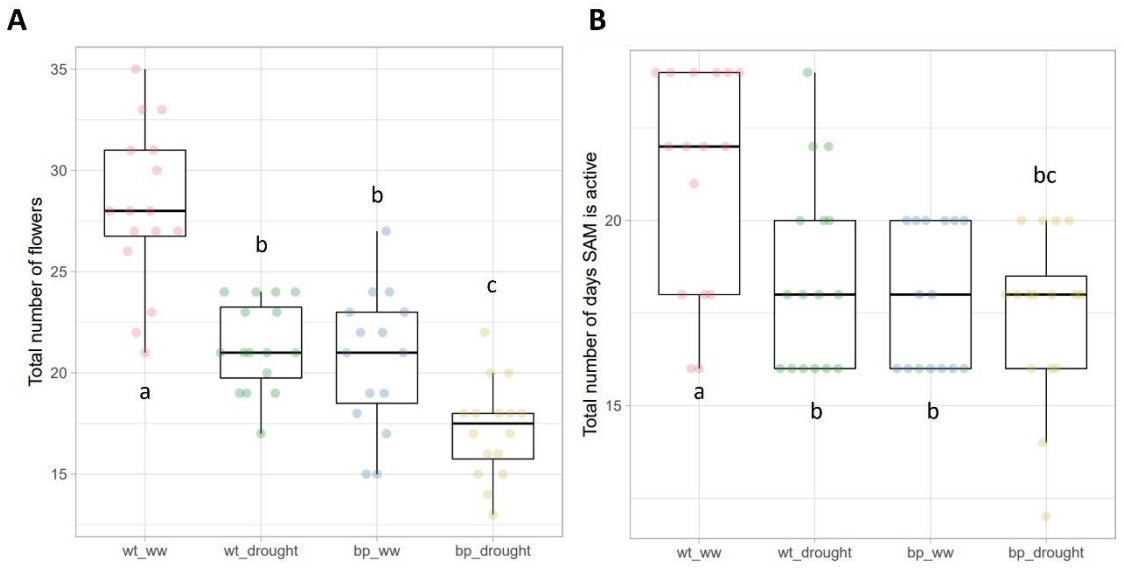

Figure 19: Boxplots represent the total number of flowers **(A)** and the total number of days in which the SAM was producing new flowers **(B)** in wt and *bp-1* plants under control and drought conditions. Dots represent independent observations. n = 16. Letters indicate significative differences between genotypes (p<0,05) by One-Way ANOVA.

4.5. Analysis of NPF4.3 activity at the SAM

4.5.1. *NPF4.3* gene edition by CRISPR/Cas9

We used the CRISPR/Cas9 genome editing system to generate *npf4.3* mutant alleles in wt and *bp-1* backgrounds. Specifically, we used the system developed by Wang et al., 2015 that allows the obtention of homozygous mutants in a single generation using the promoter of the egg cell specific *EC1.2* gene to drive the expression of Cas9 in Arabidopsis.

We designed 2 RNA guides for Cas9 activity: one guide targeting the 5' UTR of the *NPF4.3* gene and the second one targeting the second intron of *NPF4.3*. In this way, a deleted fragment of 805 base pairs spanning the first and second exons of the gene was expected (Figure 20).

In a wt background, we obtained three different alleles that contained deletions of 771, 663 and 448 base pairs, all completely removing the first two exons of the *NPF4.3* gene. In a *bp* background, we obtained lines containing the same 771 base pairs deletion that was identified in the wt.

As a result, these deletions disrupted the NPF4.3 ORF and created a new ORF of 534 base pairs, which just included the third exon of the *NPF4.3* gene (Figure 20)

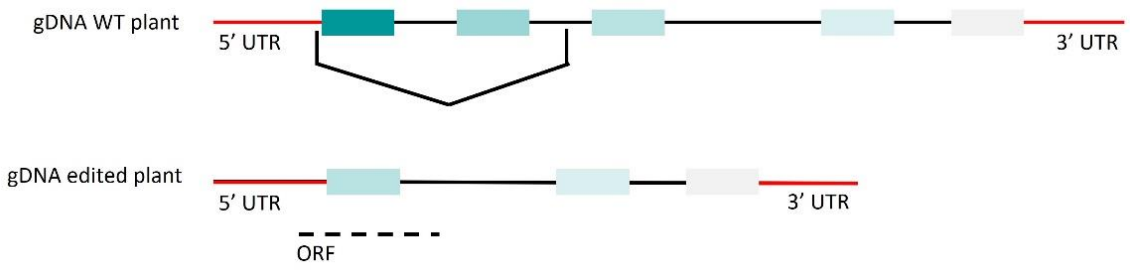

Figure 20: Schematic representation of the editions generated by CRISPR/Cas9 in the *NPF4.3* gene. Boxes indicate exons, black lines indicate introns. UTRs are coloured in red. The dashed line marks the extension of the new ORF generated by the edition.

4.5.2. SAM activity of *npf4.3* mutant lines

We carried out a preliminary characterisation of SAM activity, reported as the production of new flowers, in the novel *npf4.3* alleles generated in the wt and *bp-1* backgrounds. We analysed 3 *npf4.3* edited lines in a wt background and 2 edited lines in *bp*. All these lines carried the 771 base pairs deletion explained above, i.e. all of them included the same *npf4.3* allele. T1 lines that were homozygous for the *npf4.3* edition, but still contained the Cas9 transgene, were analysed.

If the role of NPF4.3 is to facilitate GA entry into SAM cells, we reasoned that impaired NPF4.3 activity should lower GA levels in the SAM of wt and *bp* plants. In wt plants, decreasing GA content in SAM cells could reduce flower production by stabilising DELLAs (Serrano-Mislata et al., 2017). Nevertheless, the effect of editing the *NPF4.3* gene could be masked by genetic redundancy with other members of the NPF family. In *bp*, editing *npf4.3* could restore low GA levels in SAM cells and hence wt SAM activity.

All the *npf4.3* mutant lines produced less flowers than wt plants (Figure 21), an observation that is in line with our initial hypothesis. Interestingly, the number of flowers produced by single *npf4.3* and *bp-1* mutants was similar.

bp-1 npf4.3 double mutant lines showed even lower flower production than the *bp* mutant (Figure 21). This observation may indicate that high GA levels are not the main cause of the impaired SAM activity in the *bp* mutants or that alterations of normal GA levels in SAM cells disrupt SAM activity regardless of whether GA content increases or decreases. In summary, the preliminary analysis of the *bp npf4.3* mutant highlights the complexity of the regulation of GA signalling in SAM tissues.

Importantly, the analysis of *npf4.3* edited lines presents NPF4.3 as a novel regulator of SAM activity.

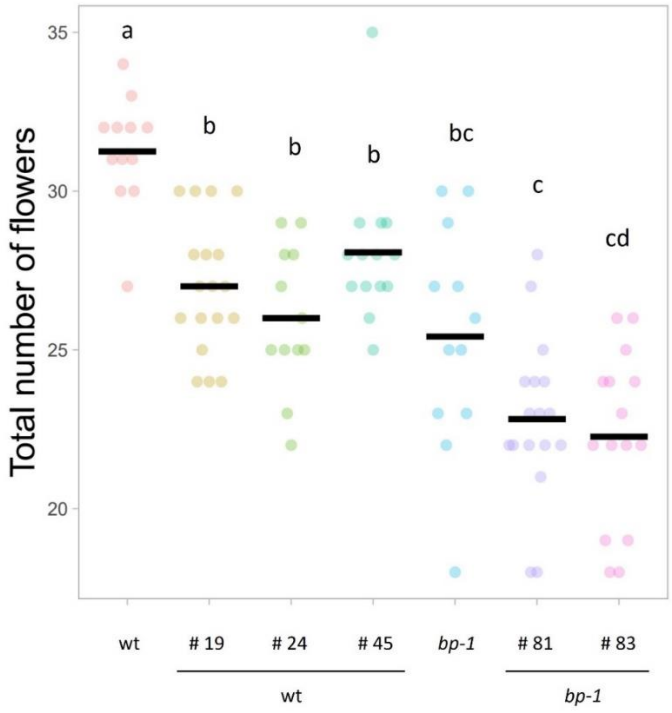

Figure 21: SAM activity represented as the cumulative number of mature flowers in the main inflorescence of wt, *bp-1*, and T1 lines including the same edition of the *NPF4.3* gene in the wt and *bp-1* backgrounds. Dots represent independent observations. Black lines indicate the average value per genotype. Letters indicate significative differences between genotypes (p<0,05) by One-Way ANOVA.

5. DISCUSSION

Cell division and cell differentiation patterns need to be precisely regulated at the SAM in order to maintain the integrity of the apical stem cells niche and to simultaneously provide cells for the development of new organs in the aerial part of plants. The environment greatly impacts this regulation. The principal interest of our group is to elucidate how environmental signals are integrated into the SAM and, especially, the response to abiotic stress conditions such as drought or salinity.

Hormone signalling pathways (CKs, GAs, ABA, auxins, etc.) transmit the environmental information to the SAM cells. This information is integrated at the SAM domain by Class I *KNOX* genes, such as *STM* and *BP*, which locally regulate hormone levels. For example, *STM* maintains a high CK/GA rate in the central region of the SAM that favours meristematic activity (Jasinski et al., 2005). Moreover, *KNOX* activity has been shown to promote the plant tolerance against certain abiotic stress conditions such as high salinity (Cai et al., 2023; Cao et al., 2023) and drought stress (Lee et al., 2016).

In order to gain insights on the role of *KNOX* genes in the integration of environmental information, the specific objective of this TFM has been to study the regulation by BP of GA signalling in the SAM.

Because of its preponderant role on SAM function, most of the previous works on KNOX activity have focused on *stm* mutants. However, working with *BP* presents some advantages as opposed to *STM*: *bp* mutants allow to study at the cellular level the development of the SAM through the different developmental stages. In contrast to *stm* mutants, which develop a bushy inflorescence with mostly vegetative organs because of early meristem termination, *bp* mutants develop a main inflorescence that produces leaves, branches, and flowers in a comparable pattern to wt plants (Endrizzi et al., 1996; Venglat et al., 2002).

Our previous work shows that *bp* SAM cells are hypersensitive to elevated GA levels, which occur for example during the floral transition. It also shows that *NPF4.3* gene expression is highly upregulated in the shoot apex of *bp* mutants (unpublished data). NPF proteins can transport different substrates, including small peptides, nitrates, sugars and the phytohormones auxins, ABA, JA and GAs. These results led us to hypothesise that BP regulates GA levels in the SAM region through the transcriptional control of *NPF4.3*.

This TFM presents some data to support this hypothesis and exemplifies the complexity of the regulation of GA signalling in SAM tissues.

Our data supports that BP is important to keep GA levels under control in SAM cells. Analysis of reporter lines showed that GA levels are normally higher in *bp* SAM cells compared to the wt. GA signalling promotes flower production through the degradation of DELLA proteins (Serrano-Mislata et al., 2017). Therefore, if the GA content is higher in bp mutants, flower production should also be higher. However, the SAM of bp mutants produced less flowers. This contradiction could be explained by the need to maintain a low but sufficient amount of GAs in the SAM, remarking the importance of a precise regulation of GA levels.

Moreover, our work supports that the SAM of bp is hypersensitive to environmental conditions that increase the GA content in the plant. Flowering in Arabidopsis is induced under long photoperiods when a peak in GA levels triggers SAM growth and the transition from the vegetative to the reproductive stage of development (Eriksson et al., 2006; Kinoshita et al., 2020). We observed that *bp* mutants flowered earlier under LD conditions, but not under SD when GA levels are lower. We have also observed that, respect to the wt, the period of flower production by the bp SAM was reduced under control conditions but not under drought stress (figure 17B). This suggests that BP regulation of SAM activity is less important under stress conditions, when bioactive GA levels in the plant decrease to stabilize the DELLA proteins that orchestrate the defence response (Colebrook et al., 2014)

In this work, we present *NPF4.3* as a novel regulator of SAM activity and relate it to GA signalling. We show that NPF4.3 locates at the plasma membrane and that it can transport GAs in yeast, as it has been described for other GA transporters such as NPF3.1 (Tal et al., 2015; Chiba et al., 2015). We also show that plants over-expressing *NPF4.3* are hypersensitive to the exogenous application of GA_3. The *NPF4.3* gene is expressed in the SAM domain and in young lateral primordia; regions with high mitotic activity where *NPF4.3* and *BP* expression domains overlap (Lincoln et al., 1994).

Impaired flower production in *npf4.3* mutants supports the idea that GA levels need to be fine-tuned in SAM cells for proper SAM activity. Reduced SAM activity in *bp* could be caused by excessive GA signalling (Jasinski et al., 2005), while reduced SAM activity in *npf4.3* and *bp npf4.3* mutants could be caused by the shortage of GAs and consequently higher levels of DELLA activity (Serrano-Mislata et al., 2017). Indeed, future experiments must include the analysis of GA and DELLA levels in *npf4.3* mutants.

In summary, we still need to prove that NPF4.3 activity is to facilitate GA entry into the SAM region, and other scenarios are still open. For example, the BP-NPF4.3 module could be controlling other signalling pathways in SAM cells, as *NPF* genes have been shown to transport small peptides, sugars, nitrates, auxins, ABA, etc. (Binembaum et al., 2018). In addition to GA

movement, BP could be controlling GA metabolism, GA perception and/or CK signalling at the SAM, as it has been described for other *KNOX* genes in different plant species (Jasinski et al., 2009; Bolduc & Hake., 2009).

6. CONCLUSIONS

1. *NPF4.3* transcript is expressed in the SAM and young lateral primordia
2. NPF4.3 locates in the plasma membrane in tobacco leaves
3. *NPF4.3* overexpression enhances the sensitivity of Arabidopsis root cells to GA_3
4. NPF4.3 can transport GA_3 in yeast assays
5. GAs levels seem to be higher in *bp*
6. *bp* mutants flower early in LD and produce less flowers
7. *npf4.3* loss of function restricts SAM activity in wt and bp plants

7. REFERENCES

Byrne, M. E., Simorowski, J., & Martienssen, R. A. (2002). ASYMMETRIC LEAVES1 reveals knox gene redundancy in Arabidopsis

Cai, H., Xu, Y., Yan, K., Zhang, S., Yang, G., Wu, C., ... & Huang, J. (2023). BREVIPEDICELLUS Positively Regulates Salt-Stress Tolerance in Arabidopsis thaliana. *International Journal of Molecular Sciences*, *24*(2), 1054.

Cao, X., Du, Q., Guo, Y., Wang, Y., & Jiao, Y. (2023). Condensation of STM is critical for shoot meristem maintenance and salt tolerance in Arabidopsis. *Molecular Plant*, *16*(9), 1445-1459.

Chiba, Y., Shimizu, T., Miyakawa, S., Kanno, Y., Koshiba, T., Kamiya, Y., & Seo, M. (2015). Identification of Arabidopsis thaliana NRT1/PTR FAMILY (NPF) proteins capable of transporting plant hormones. *Journal of plant research*, *128*, 679-686.

Colebrook, E. H., Thomas, S. G., Phillips, A. L., & Hedden, P. (2014). The role of gibberellin signalling in plant responses to abiotic stress. *Journal of experimental biology*, *217*(1), 67-75.

Davière, J. M., & Achard, P. (2013). Gibberellin signaling in plants. *Development*, *140*(6), 1147-1151.

Endrizzi, K., Moussian, B., Haecker, A., Levin, J. Z., & Laux, T. (1996). The SHOOT MERISTEMLESS gene is required for maintenance of undifferentiated cells in Arabidopsis shoot and floral meristems and acts at a different regulatory level than the meristem genes WUSCHEL and ZWILLE. *The plant journal*, *10*(6), 967-979.

Eriksson, S., Böhlenius, H., Moritz, T., & Nilsson, O. (2006). GA4 is the active gibberellin in the regulation of LEAFY transcription and Arabidopsis floral initiation. *The Plant Cell*, *18*(9), 2172-2181.

Ferrandiz, C., Liljegren, S. J., & Yanofsky, M. F. (2000). Negative regulation of the SHATTERPROOF genes by FRUITFULL during Arabidopsis fruit development. *Science*, *289*(5478), 436-438.

Gaillochet, C., Daum, G., & Lohmann, J. U. (2015). O cell, where art thou? The mechanisms of shoot meristem patterning. *Current opinion in plant biology*, *23*, 91-97.

Ha, C. M., Jun, J. H., & Fletcher, J. C. (2010). Shoot apical meristem form and function. *Current topics in developmental biology*, *91*, 103-140.

Hay, A., Kaur, H., Phillips, A., Hedden, P., Hake, S., & Tsiantis, M. (2002). The gibberellin pathway mediates KNOTTED1-type homeobox function in plants with different body plans. *Current Biology*, *12*(18), 1557-1565.

Janocha, D., & Lohmann, J. U. (2018). From signals to stem cells and back again. *Current opinion in plant biology*, *45*, 136-142.

Jasinski, S., Piazza, P., Craft, J., Hay, A., Woolley, L., Rieu, I., ... & Tsiantis, M. (2005). KNOX action in Arabidopsis is mediated by coordinate regulation of cytokinin and gibberellin activities. *Current Biology*, *15*(17), 1560-1565.

Khakhar, A., Leydon, A. R., Lemmex, A. C., Klavins, E., & Nemhauser, J. L. (2018). Synthetic hormone-responsive transcription factors can monitor and re-program plant development. *Elife*, *7*, e34702.

Kinoshita, A., Vayssières, A., Richter, R., Sang, Q., Roggen, A., van Driel, A. D., ... & Coupland, G. (2020). Regulation of shoot meristem shape by photoperiodic signaling and phytohormones during floral induction of Arabidopsis. *Elife*, *9*, e60661.

Lee, H. G., Choi, Y. R., & Seo, P. J. (2016). Increased STM expression is associated with drought tolerance in Arabidopsis. *Journal of plant physiology*, *201*, 79-84.

Li, G., Manzoor, M. A., Wang, G., Chen, C., & Song, C. (2023). Comparative analysis of KNOX genes and their expression patterns under various treatments in Dendrobium huoshanense. *Frontiers in Plant Science*, *14*.

Lincoln, C., Long, J., Yamaguchi, J., Serikawa, K., & Hake, S. (1994). A knotted1-like homeobox gene in Arabidopsis is expressed in the vegetative meristem and dramatically alters leaf morphology when overexpressed in transgenic plants. *The Plant Cell*, *6*(12), 1859-1876.

Long, J. A., Moan, E. I., Medford, J. I., & Barton, M. K. (1996). A member of the KNOTTED class of homeodomain proteins encoded by the STM gene of Arabidopsis. *Nature*, *379*(6560), 66-69.

Ma, X., Sukiran, N. L., Ma, H., & Su, Z. (2014). Moderate drought causes dramatic floral transcriptomic reprogramming to ensure successful reproductive development in Arabidopsis. *BMC Plant Biology*, *14*(1), 1-16.

Park, J., Lee, Y., Martinoia, E., & Geisler, M. (2017). Plant hormone transporters: what we know and what we would like to know. *BMC biology*, *15*, 1-15.

Ragni, L., Belles-Boix, E., Gunl, M., & Pautot, V. (2008). Interaction of KNAT6 and KNAT2 with BREVIPEDICELLUS and PENNYWISE in Arabidopsis inflorescences. *The Plant Cell*, *20*(4), 888-900.

Richards, D. E., King, K. E., Ait-Ali, T., & Harberd, N. P. (2001). How gibberellin regulates plant growth and development: a molecular genetic analysis of gibberellin signaling. *Annual review of plant biology*, *52*(1), 67-88.

Sakamoto, T., Kamiya, N., Ueguchi-Tanaka, M., Iwahori, S., & Matsuoka, M. (2001). KNOX homeodomain protein directly suppresses the expression of a gibberellin biosynthetic gene in the tobacco shoot apical meristem. *Genes & development*, *15*(5), 581-590.

Serrano-Mislata, A., Bencivenga, S., Bush, M., Schiessl, K., Boden, S., & Sablowski, R. (2017). DELLA genes restrict inflorescence meristem function independently of plant height. *Nature Plants*, *3*(9), 749-754.

Shi, B., & Vernoux, T. (2019). Patterning at the shoot apical meristem and phyllotaxis. *Current topics in developmental biology*, *131*, 81-107.

Silverstone, A. L., Jung, H. S., Dill, A., Kawaide, H., Kamiya, Y., & Sun, T. P. (2001). Repressing a repressor: gibberellin-induced rapid reduction of the RGA protein in Arabidopsis. *The Plant Cell*, *13*(7), 1555-1566.

Su, Z., Ma, X., Guo, H., Sukiran, N. L., Guo, B., Assmann, S. M., & Ma, H. (2013). Flower development under drought stress: morphological and transcriptomic analyses reveal acute responses and long-term acclimation in Arabidopsis. *The Plant Cell*, *25*(10), 3785-3807.

Tal, I., Zhang, Y., Jørgensen, M. E., Pisanty, O., Barbosa, I. C., Zourelidou, M., ... & Shani, E. (2016). The Arabidopsis NPF3 protein is a GA transporter. *Nature communications*, *7*(1), 11486.

Traas, J., & Vernoux, T. (2002). The shoot apical meristem: the dynamics of a stable structure. *Philosophical Transactions of the Royal Society of London. Series B: Biological Sciences*, *357*(1422), 737-747.

Venglat, S. P., Dumonceaux, T., Rozwadowski, K., Parnell, L., Babic, V., Keller, W., ... & Datla, R. (2002). The homeobox gene BREVIPEDICELLUS is a key regulator of inflorescence architecture in Arabidopsis. *Proceedings of the National Academy of Sciences*, *99*(7), 4730-4735.

Wang, Z. P., Xing, H. L., Dong, L., Zhang, H. Y., Han, C. Y., Wang, X. C., & Chen, Q. J. (2015). Egg cell-specific promoter-controlled CRISPR/Cas9 efficiently generates homozygous mutants for multiple target genes in Arabidopsis in a single generation. *Genome biology*, *16*, 1-12.

Zhao, M., Yang, S., Chen, C. Y., Li, C., Shan, W., Lu, W., ... & Wu, K. (2015). Arabidopsis BREVIPEDICELLUS interacts with the SWI2/SNF2 chromatin remodeling ATPase BRAHMA to regulate KNAT2 and KNAT6 expression in control of inflorescence architecture. *PLoS genetics*, *11*(3), e1005125.